OPEN

Paper

Potential Airborne Releases and Deposition of Radionuclides from the Santa Susana Field Laboratory during the Woolsey Fire

Arthur S. Rood,[1] H. Justin Mohler,[2] Helen A. Grogan,[3] Colby Mangini,[4] Emily A. Caffrey,[5] and John E. Till[6]

Abstract—**The Santa Susana Field Laboratory (SSFL), located in southern California, is a former research facility, and past activities have resulted in residual radioactive contamination in Area IV of the Site. The Woolsey Fire burned across the site, including some of the contaminated areas, on 8–11 November 2018. Atmospheric transport modeling was performed to determine where the smoke plume went while the fire burned across the SSFL and the deposition footprint of particulates in downwind communities. Any radionuclides on vegetation and in surface soil released by the fire were assumed to follow particulate matter transport path and deposition. The predicted deposition footprint was used to guide confirmatory soil sampling at 16 locations including background. Highest offsite deposition was determined to be northeast of the Oak Park community, which is located about 6 km southwest of SSFL. Depth-profile sampling was used to evaluate whether radionuclides of SSFL origin were potentially emitted and deposited during the Woolsey Fire. If radionuclides had been deposited from the Woolsey Fire at sufficient concentrations, then they would be detected in the surface layer and would be expected to be higher within the plume footprint than outside it. An upper bound estimate of the hypothetical effective dose to a person in Oak Park based on measured radionuclide concentrations in soil and vegetation on the SSFL was less than 0.0002 mSv. The occurrence of naturally occurring radionuclides at concentrations above the established background for the SSFL was attributed to natural variability in geologic formations and not SSFL. No anthropogenic radionuclides were measured at levels above those expected from global fallout. The soil sampling confirmed that no detectable levels of SSFL-derived radionuclides migrated from SSFL at the locations sampled because of the Woolsey Fire or from past operations of the SSFL.**

[1]K-Spar, Inc., 4835 W Foxtrail Lane, Idaho Falls, ID 83402; [2]Bridger Scientific, Inc., 125 Jackpot Lane, Belgrade, MT 59714; [3]Cascade Scientific, Inc., 1678 NW Albany Avenue, Bend, OR 97703; [4]Paragon Scientific, 725 Rucker Avenue, Everett, WA 98201; [5]Radian Scientific LLC, 806 Wells Ave SE, Huntsville, AL 35801; [6]Risk Assessment Corporation, 417 Till Road, Neeses, SC 29107.

For correspondence contact: Arthur Rood, K-Spar, Inc., 4835 W Foxtrail Lane, Idaho Falls, ID 83402, or email at **asr@kspar.net**.

(*Manuscript accepted* 16 *October* 2022)

0017-9078/23/0

DOI: 10.1097/HP.0000000000001665

Health Phys. 124(4):257–284; 2023

Key words: modeling, meteorological; monitoring, environmental; geology; radioactivity, environmental

INTRODUCTION

The Santa Susana Field Laboratory (SSFL or site) is located between the San Fernando Valley and Simi Valley in Ventura County in southern California (Fig. 1). Historic site operations at SSFL included rocket engine testing and energy research, including liquid metals and nuclear power. Most nuclear research and related programs ceased in 1988, and all rocket engine testing operations at SSFL ceased in 2006. Almost all buildings and structures at SSFL have been decommissioned and demolished, and the site is currently undergoing remediation of contamination caused by past industrial activities. On 8 November 2018, the Woolsey Fire started in the Woolsey Canyon area south of Simi Valley in Ventura County. It was reported to have ignited near the northern boundary of the SSFL (Citygate 2019) and burned quickly across a portion of the site pushed by the powerful Santa Ana winds. The Woolsey Fire was declared 100% contained on 21 November 2018 (DTSC 2020).

The purpose of this work was: (1) to determine if detectable levels of SSFL-derived radionuclides migrated from SSFL and could be detected in offsite soils because of the Woolsey Fire burning across SSFL, and (2) if so, what would be the hypothetical annual effective dose to a person exposed to both the airborne smoke plume during the fire burning at SSFL and subsequently to material deposited on the ground surface?

The progression of the Woolsey Fire across the SSFL was modeled to aid in the design of a soil-sampling plan to look for potential impacts from the fire and to confirm modeling results. Sampling locations were identified based on the modeled plume of particulate matter emitted from the fire and the areas that were predicted to be impacted by deposition of particulates from the smoke plume that originated from the fire burning at the SSFL. These locations included downwind areas where atmospheric deposition of

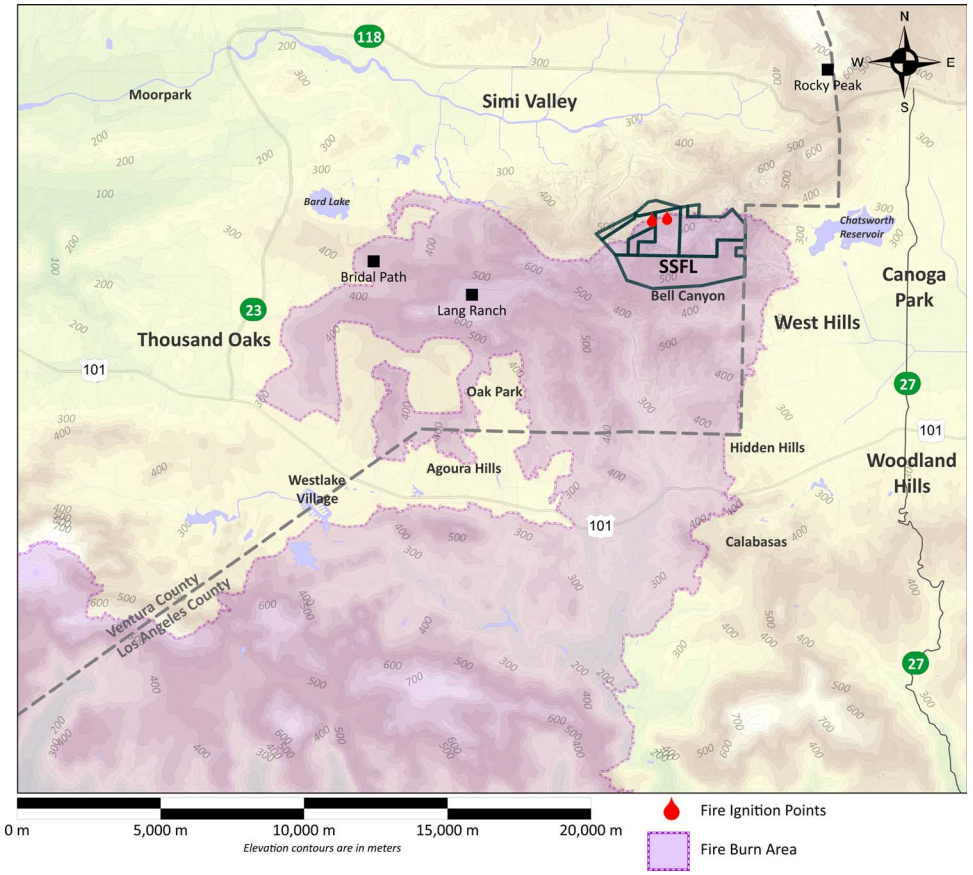

Fig. 1. Study region around the Santa Susana Field Laboratory (SSFL) showing the Woolsey Fire burn area, suspected fire ignition points, and EPA background sample locations identified as Bridal Path, Lang Ranch, and Rocky Peak. The extent of the Woolsey Fire burn area was obtained from LA County (2019).

particulates was anticipated to be largest, as well as locations that were outside the deposition plume of the fire and thus would have remained unimpacted. The analysis draws upon environmental monitoring data collected before, during, and after the Woolsey Fire.

Overview of the SSFL

The SSFL began operations in 1947 on land acquired by North American Aviation (NAA) in the Simi Hills between Simi Valley and San Fernando Valley. The SSFL site has a total area of 11.5 km^2 (2,850.5 acres). The facility's mission initially was rocket engine testing. In 1955, a portion of SSFL (1.17 km^2, 289.9 acres), known as Area IV, located in the northwestern corner of the site, was set aside for nuclear research and testing by Atomics International, then a division of NAA (Fig. 2). In 1984, Atomics International merged with Rocketdyne, a division of Rockwell International, which was acquired in 1996 by The Boeing Company (Boeing). Boeing subsequently sold Rocketdyne in 2005. Today Boeing owns Areas I, III, IV, and the undeveloped land of SSFL (9.71 km^2, 2,399.3 acres). Approximately 0.36 km^2 (90 acres) of Area IV was leased to the US Department of Energy (US DOE) and its predecessor agencies in the past for nuclear research activities. A portion of the site (1.83 km^2, 451.2 acres), Area II, is owned by the federal government and is administered by the National Aeronautics and Space Administration (NASA). Area II is used by NASA and the Department of Defense (US DOD) for rocket engine and laser testing.

The US DOE's Energy Technology Engineering Center (ETEC) was in Area IV and was comprised of a group of government-owned facilities used for nuclear research and development, as well as research and testing of non-nuclear components related to liquid metals. From the mid-1950s until 1988, nuclear operations included the construction and operation of nuclear research reactors; the fabrication, disassembly, and examination of nuclear reactor fuel; and other radioactive materials research sponsored by US DOE and its predecessor agencies. Nuclear operations at the ETEC included 10 nuclear research reactors and seven critical facilities. These facilities included the Hot Laboratory, the Nuclear Materials Development Facility, the Radioactive Materials Handling Facility, and various radioactive material storage areas.

The Sodium Reactor Experiment (SRE) located in Area IV malfunctioned in July 1959 because of a partial blockage of the sodium coolant in some of the reactor

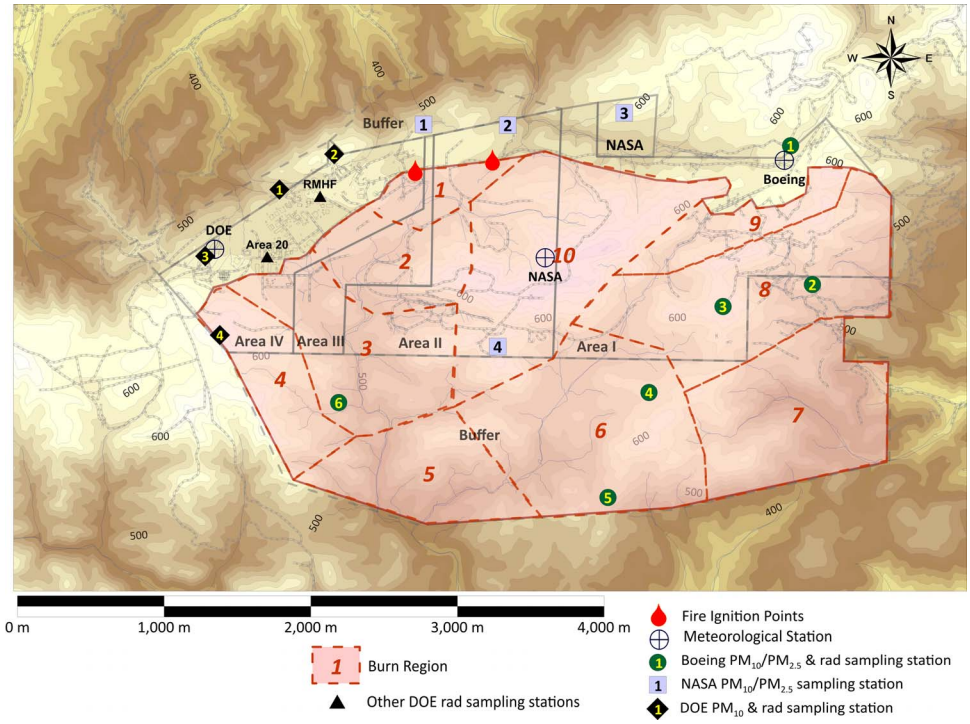

Fig. 2. SSFL showing administrative areas (Areas I through IV), particulate sampler locations, meteorological stations, and the 10 burn regions starting from region (1) on 8 November 2018, at 14:30 PST (rounded to the nearest half-hour) and ending with region (10). Active fire burning on SSFL ceased on the early morning of 11 November 2018, but all regions smoldered for some time after active burning.

coolant channels. The blockage resulted in the partial melting of 13 of the 43 reactor fuel assemblies and the release of fission products to the primary reactor cooling system and some of the inside rooms of the facility. The reactor was safely shut down, and the primary pressure vessel remained intact. All gases released from the incident were captured inside the building. Noble gases (^{85}Kr and ^{135}Xe) were released in a controlled manner to the atmosphere over a period of time and in compliance with airborne release limits; however, all other fission products, notably ^{137}Cs and ^{131}I, were retained in the sodium coolant and removed during cleanup operations. Environmental monitoring data for 1959 showed no increase in radioactivity after the incident in air, soil, or water (AI 1960). The reactor was cleaned, repaired, and continued operation until 1964 when the program ended (Boeing 2021).

Most nuclear research activities in Area IV ended in 1988. Activities conducted at the ETEC have resulted in soil contamination in Area IV. The DOE is responsible for remediation of soil contamination in Area IV and the Northern Buffer Zone. At the time of the Woolsey Fire in 2018, some of the contaminated soils had been excavated and removed, and most buildings had been decommissioned and removed.

MATERIALS AND METHODS

Investigation of potential releases and impacts from the Woolsey Fire burning across the SSFL involved first understanding the fire progression timeline followed by development of an atmospheric transport model simulation of the fire. Environmental monitoring data were reviewed and used in conjunction with dispersion factors developed from the atmospheric transport modeling to estimate potential radionuclide fallout from the fire, the dose to a hypothetical individual, and the minimum detectable dose from the confirmatory soil sampling that followed.

The Woolsey Fire

The Woolsey Fire was reported to have begun on 8 November 2018 at 14:24 Pacific Standard Time (PST) near a Southern California Edison substation located along the northern boundary of the SSFL (Fig. 2) (Citygate 2019). A second ignition point ~500 m west of the first ignition point was also identified. The fire quickly spread to the southwest pushed by strong Santa Ana winds reaching speeds of about 21 m s^{-1} (47 mph), as measured at the SSFL. The fire spread off-site during the late afternoon/evening and was reported to be burning near the community of Oak Park at 21:00 PST the evening of 8 November (Citygate 2019). The fire jumped U.S. Route 101 between Liberty Canyon Road and Palo Comado Canyon Road overpass at 05:13 PST on 9 November (Citygate 2019). During the day of 9 November, the fire spread rapidly westward (Citygate 2019) and to portions of Thousand Oaks, Bell Canyon, Westlake Village, and West Hills (Wildfire Today 2019). The Woolsey Fire burned approximately 80% of

the SSFL. The Woolsey Fire was declared 100% contained on 21 November 2018 at 18:11 PST (DTSC 2020).

A timeline of the Woolsey Fire activity on the SSFL was constructed using different sources of information including meteorological data, video from webcams located at Boeing air monitoring stations, and details regarding the fire progression (Fig. 2 and Table 1). Ten distinct regions were identified by date and time of burning. Initially, the fire burned toward the southwest from the two ignition points and crossed the western boundary of the SSFL during the late afternoon/evening of 8 November. During the late evening of 8 November to the early morning of 9 November, a portion of the Woolsey Fire burned offsite through Bell Canyon, which borders the southern boundary of SSFL (Citygate 2019). Around 22:00 PST on 9 November, a portion of the fire located offsite to the south of SSFL burned toward the north back onto SSFL, and then moved back toward the west and offsite in the early morning of 10 November. Areas of burning continued during 10 November and active burning at the SSFL ceased by the morning of 11 November 2018.

Source term

Radionuclides potentially present in vegetation and surface soil would be released with the burning of vegetation and the suspension of soil in a similar manner that particulate matter is released from a fire (Grogan et al. 2007). Thus, development of a radionuclide source term first involved estimating particulate releases from the fire. A fraction of the particulate matter that is released to the atmosphere will deposit from the plume on the soil as it is transported downwind. Likewise, any radionuclides in particulate form entrained in the plume would also deposit on the soil as they are transported downwind.

Each region of the Woolsey Fire on SSFL was modeled using the Fire Emission Production Simulator (FEPS) Version 1.1.0 (Anderson et al. 2004) computer program. This model takes as input the beginning and ending time of the fire, the area burned, fuel loading, relative humidity, wind speed, temperature, and atmospheric stability. Fuel loading is defined from the National Fire Danger Rating System 1978 Fuel Model Definitions (Deeming et al. 1977). Fuel model B was selected for the model because it represents California's mixed chaparral ecosystem that covers the SSFL. Dominant plant species in a mixed chaparral ecosystem include scrub oak, chaparral oak, and several species of ceanothus and manzanita (Ornduff 1974). The default fuel loads for this material are 11.5 tons per acre of shrub, 4.5 tons per acre of woody material, and 3.5 tons per acre of litter (Deeming et al. 1977).

The fuel condition was assumed to be very dry based on the meteorological conditions recorded at the Boeing and NASA meteorological towers. The FEPS default moisture percentages for very dry fuels are 4%, 6%, 8%, and 8% for the 1-h, 10-h, 100-h, and 1,000-h times, respectively. The FEPS default moisture percentage was 60% for live material and 25% litter. Wind speed, relative humidity, and temperature were obtained from the Boeing meteorological tower located in the northeast corner of the SSFL (Fig. 2). Hourly average windspeeds increased from about 2 m s^{-1} (4.5 mph) to over 8 m s^{-1} (18 mph) about an hour before the fire started. Gusts of over 20 m s^{-1} (45 mph) were measured during this period, and relative humidity dropped from over 96% to about 6%. Temperatures were relatively mild for Santa Ana conditions with a maximum of about 22 °C (~72 °F) recorded on 10 November 2018. Atmospheric stability was estimated for each hour based on Pasquill-Gifford classification using Turner's method (Turner 1964). High wind speeds and clear skies resulted in neutral stability conditions for most of the time the fire burned on SSFL.

The total area of each fire region on the SSFL was divided by the number of hours the region actively burned to provide the consumption rate that was entered into FEPS (i.

Table 1. Fire Regions on the SSFL, area burned, and date and time.

Region ID[a]	Area (m^2)	Area (acres)	Consumption rate (acres h^{-1})	Date and time (PST)[b]
1	206,502.7	51.0	34.0	11/08/2018, 14:30–16:00
2	576,969.7	142.6	35.6	11/08/2018, 16:00–20:00
3	988,611.0	244.3	244.3	11/08/2018, 20:00–21:00
4	549,912.6	135.9	135.9	11/08/2018, 2100–2200
5	730,145.4	180.4	180.4	11/08/2018 22:00–23:00
6	1,509,361.7	373.0	124.3	11/09/2018 00:00–03:00
7	1,144,709.9	282.9	40.4	11/09/2018 03:00–10:00
8	1,477,440.3	365.1	73.0	11/09/2018 10:00–15:00
9	373,000.4	92.2	11.5	11/09/2018 15:00–23:00
10	1,620,482.3	400.4	14.3	11/10/2018, 00:00 to 11/11 04:00

[a] See Fig. 2.

[b] Pacific Standard Time.

e., acres per hour or tons of fuel per hour). Region 3, which burned during the highest recorded wind speeds, had the highest burn rate (see Table 1). Lower burn rates corresponded to periods of relatively light wind speeds, which were recorded on the evening of the 9 November 2018 and on the morning of 10 November 2018. Separate modeling was performed for each region of the Woolsey Fire on the SSFL and assumed linear growth of the Woolsey Fire across each region. The estimated emission rate for particulate matter with diameters less than 2.5 μm ($PM_{2.5}$) from all sources as a function of time (Fig. 3) shows that the highest emission rates occurred in the late afternoon and evening of 8 November 2018 and the early morning of 9 November 2018 during the period of highest wind speeds.

The FEPS model produces emission estimates as a function of time for carbon monoxide, methane, and $PM_{2.5}$ (particulate matter with diameters less than 2.5 μm). For this application, only the $PM_{2.5}$ was included in the atmospheric dispersion model because measurements at the Boeing air samplers included both $PM_{2.5}$ and PM_{10} (particulate matter with diameters less than 10 μm).

Atmospheric transport modeling

The purpose of the atmospheric transport modeling was to estimate the deposition pattern of particulate matter and any associated radionuclides from the Woolsey Fire while it burned on the SSFL. The transport and deposition of particulate matter was modeled using the CALPUFF (Scire et al. 2000) modeling system Version 7 (Exponent 2019). CALPUFF is an advanced non-steady-state meteorological and air quality modeling system used to compute particulate and gaseous concentrations of material emitted to the atmosphere. Version 7 includes an interface between FEPS and CALPUFF so that the output from FEPS can be processed and used directly in a CALPUFF simulation. The CALPUFF modeling system consists of three primary codes: a meteorological model (CALMET), a complex terrain Lagrangian puff dispersion model (CALPUFF), and a post-processing program (CALPOST). There are also numerous preprocessors for developing input data that include surface and upper air meteorological data, terrain and land-use data, and the source-term data provided by FEPS.

Model domain and discretization

The model domain measured 33.1 km east-west by 27.5 km north-south covering an area of 910.26 km^2 (224,928 acres) (see Fig. 1). Terrain in the SSFL region is characterized as complex and rugged. Elevations above mean sea level within the model domain ranged from 55 m to 917 m, with a median elevation of 331 m. The rugged terrain required a refined horizontal grid spacing of 100 m, resulting in 332 east-west nodes and 276 north-south nodes for a total of 91,632 nodes. The 100-m grid spacing allowed the steep terrain in the vicinity of the SSFL to be accounted for by the model.

The atmosphere was discretized into 10 vertical layers having upper bounds of 20 m, 40 m, 80 m, 160 m, 320 m, 640 m, 1,200 m, 2,000 m, 3,000 m, and 4,000 m above ground surface.

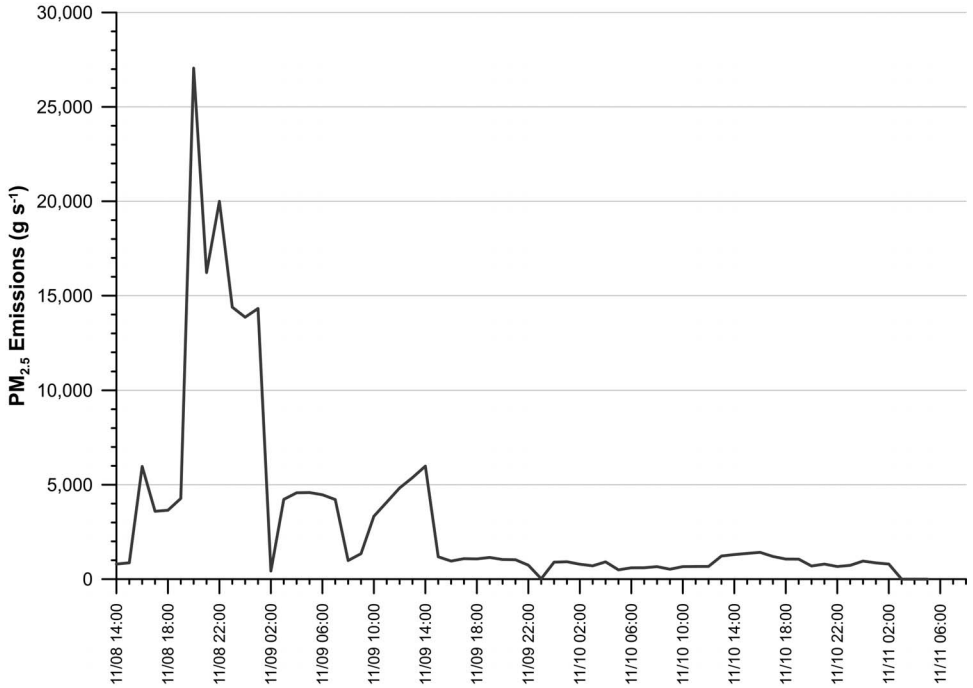

Fig. 3. FEPS-predicted release rate of $PM_{2.5}$ as a function of time from Woolsey Fire burning on the SSFL.

Meteorological data

Meteorological towers on the SSFL are illustrated in Fig. 2. Boeing operates the tower in the northeastern corner of the facility. NASA operates the tower near the center of the facility, and DOE operates the tower in the northwest portion of the facility. The DOE tower was inoperable during the fire and thus provided no data for the model simulation. The Boeing and NASA towers remained operational during the fire and were the primary source of on-site meteorological data. Wind speed and direction were measured at 10 m or 15 m, which is optimal for surface measurements and generally recommended by the US Environmental Protection Agency (US EPA).

Boeing also measures windspeed and direction at six particulate air monitoring stations that are identified in Fig. 2. These measurements are made at the 2-m level and supplemented data from the towers.

Meteorological data from the towers at the Burbank and Van Nuys airports were also obtained and used in the simulation. Although these stations are outside the model domain, they provided required data on cloud cover and barometric pressure. Cloud cover and barometric pressure were not likely to differ from conditions at the SSFL, especially during Santa Anna conditions. CALMET also requires upper air sounding from the nearest upper air station, which is at Vandenberg AFB. The twice daily soundings during the fire were obtained and used in the simulation.

Wind roses during the most active burning period of the fire at the two operational towers and the six Boeing air monitoring locations show winds predominantly out of the north-northeast to northeast direction; however, the Boeing main tower had winds predominately out of the east-northeast, and Boeing station 4 had winds predominantly out of the north. It is likely that terrain channeling influenced the wind direction at Boeing station 4. Wind speeds were highest at the NASA tower, which is at the highest elevation of all the stations. Wind speeds for the Boeing air monitoring stations (2-m measurement height) generally exhibited lower windspeeds than the meteorological towers as expected. The Boeing main tower and Boeing monitoring station 1 are relatively close to each another but exhibited different predominant wind directions. This observation is likely due to different measurement heights and the turbulent nature of the winds during the fire.

CALPUFF model options

In general, default technical options and parameters were used in the CALMET and CALPUFF simulations. Model parameters and options with no default value or where the default was not selected are discussed below.

The bias variable weights the surface and upper air readings in the wind field interpolation scheme. A bias value of −1 reduces the weight of the upper air stations by 100%, and a bias value of 1 reduces the weight of a surface station by 100%. Bias variable values range between −1 and 1 (i.e., a bias value of −0.3 weights the upper air observations by 30% and applies a weight of 70% to the surface stations). In this application, a gradational approach was used (as recommended in CALPUFF) so that at the surface layer, the surface stations are weighted by 100%; in the uppermost layer, the upper air station is weighted by 100%. Bias values for each layer from the surface to the highest layer were − 1, −0.9, −0.8, −0.7, −0.4, 0.0, 0.7, 1.0, 1.0, 1.0.

The CALMET default is to use all stations weighted by the distance squared. Because conditions can vary significantly across the SSFL, the varying radius of influence option was used in the simulation. For surface stations, all stations within 2 km of the model grid point were used in the wind field interpolation. If no stations were found within 2 km, then the nearest station was used. For upper air stations, the radius value was 100 km because only one station was used. Radius of influence for terrain features was 0.5 km. That is, terrain features within 0.5 km of a grid point were included in the simulation. Observations within 0.5 km of a grid point were given equal weighting between the observation and the first-guess wind field as prescribed in CALMET.

For kinematic effects (the change in air properties due to the advection of air parcels), a non-default option in CALMET was selected because of the strong and chaotic nature of Santa Ana winds that drove the fire.

The dispersion coefficients used in the CALPUFF simulation were determined from internally calculated micrometeorological variables that account for the physical and dynamic occurrences within a shallow stratum of air adjacent to the ground and provide a non-biased estimate of air concentrations. This represents the current state-of-the art in atmospheric dispersion modeling.

Predicted and observed $PM_{2.5}$ concentrations

Boeing, NASA, and US DOE operate a total of 14 PM_{10} monitors on the SSFL, and at three stations (Boeing stations 1 and 4, NASA station 2) there is also a $PM_{2.5}$ monitor (Fig. 2). Data before, during and after the fire were obtained electronically from NASA and Boeing, and US DOE data from North Wind (2019a and b). Particulate matter emission is a natural consequence of wildfires, and the measurements showed a clear increase in particulate matter concentrations during the Woolsey Fire. The response of the PM_{10} samplers is consistent with the fire progression. High particulate matter concentrations (Table 2 and Table 3) corresponded to times at which smoke and suspended materials were known to be present, demonstrating that the samplers captured the impacts of the fire.

The CALPUFF simulation calculates the 24-h average $PM_{2.5}$ concentration at each of the monitoring stations from $PM_{2.5}$ emitted while the Woolsey Fire burned in the different

Table 2. Measured and predicted net 24-h average $PM_{2.5}$ concentrations at the Boeing samplers ($\mu g\ m^{-3}$).

Date	Measured Boeing 1	Measured[b] Boeing 2	Measured[b] Boeing 3	Measured Boeing 4	Measured[b] Boeing 5	Measured[b] Boeing 6
11/8/2018	7.9	37.2	22.4	19.5	23.8	299.9
11/9/2018	4.0	338.6	301.8	436.1	450.3	79.9
11/10/2018	43.7	24.1	20.1	48.8	34.8	20.7
11/11/2018	15.2	41.4	41.6	22.5	33.1	31.6
Average	17.7	110.3	96.5	131.7	135.5	108.0
Average measured over all samplers: 100 $\mu g\ m^{-3}$						
Date	Predicted Boeing 1	Predicted Boeing 2	Predicted Boeing 3	Predicted Boeing 4	Predicted Boeing 5	Predicted Boeing 6
11/8/2018	11.7	11.7	11.7	11.7	12.2	259.2
11/9/2018	38.6	150.4	52.1	102.1	61.2	26.1
11/10/2018	17.5	23.3	33.6	241.3	37.3	74.0
11/11/2018	11.7	11.7	11.9	14.6	15.0	12.4
Average	19.8	49.3	27.3	92.4	31.4	92.9
Average predicted over all samplers: 52.2 $\mu g\ m^{-3}$						
P/O[a]	1.1	0.45	0.28	0.70	0.23	0.86

P/O of sampler average: 0.52

[a] Predicted-to-observed (measured) ratio of sampler time average.

[b] Calculated from PM_{10} measurement based a PM_{10} to $PM_{2.5}$ ratio of 2.05.

areas of the SSFL. Because the CALPUFF-predicted concentration represents a net value that does not include the contribution from background, the average background $PM_{2.5}$ concentration (11.7 $\mu g\ m^{-3}$) was added to the predicted concentration at each location for comparison to the measured concentration. The background $PM_{2.5}$ concentration was calculated from pre-fire data measured at Boeing stations 1 and 4 and NASA station 2. The pre-fire Boeing data spanned from 15 April 2018 to the start of the Woolsey Fire and the pre-fire NASA data spanned from 1 November 2018 to the start of the Woolsey Fire. For stations that only measured PM_{10}, the $PM_{2.5}$ concentration was estimated by dividing the PM_{10} concentration by the average PM_{10} to $PM_{2.5}$ ratio measured during the fire (2.05).

Predicted and measured $PM_{2.5}$ concentrations (Table 2, Table 3, and Table 4) show that predicted (*P*) concentrations are approximately within a factor of 2 of the observations (*O*) (i.e., overpredict or underpredict the measured concentration by a factor of 2). Atmospheric transport model predictions within a factor of 2 of the observations are generally considered acceptable model performance (Chang and Hanna 2004). Previous modeling studies of wildfires show

Table 3. Measured and predicted net 24-h average $PM_{2.5}$ concentrations at the NASA Samplers ($\mu g\ m^{-3}$).

Date	Measured [b] NASA 1	Measured NASA 2	Measured [b] NASA 3	Measured [b] NASA 4
11/8/2018	28.0	16.4	26.0	27.7
11/9/2018	11.1	5.0	8.1	363.8
11/10/2018	15.8	75.6	28.8	25.7
11/11/2018	17.7	19.0	13.0	31.0
Average	18.2	29.0	19.0	112.1
Average measured over all samplers: 44.5 $\mu g\ m^{-3}$				
Date	Predicted NASA 1	Predicted NASA 2	Predicted NASA 3	Predicted NASA 4
11/8/2018	11.7	11.7	11.7	12.0
11/9/2018	16.6	16.4	17.4	39.7
11/10/2018	25.4	18.4	17.4	110.9
11/11/2018	11.8	11.8	11.8	24.0
Average	16.4	14.6	14.6	46.7
Average predicted over all samplers: 23 $\mu g\ m^{-3}$				
P/O[a]	0.90	0.50	0.77	0.42

P/O of sampler average: 0.52

[a]Predicted-to-observed (measured) ratio of sampler time average.

[b]Calculated from PM_{10} measurement based on a PM_{10} to $PM_{2.5}$ ratio of 2.05.

Table 4. Measured and predicted net 24-h average $PM_{2.5}$ concentrations at the US DOE Samplers ($\mu g\ m^{-3}$).

Date	Measured [c] DOE 1	Measured [c] DOE 2	Measured [c] DOE 3	Measured [c] DOE 4
11/8/2018	27.0	32.3	25.1	b
11/9/2018	11.5	14.9	14.9	b
11/10/2018	10.7	10.5	12.3	b
11/11/2018	14.8	14.1	14.9	b
Average	16.0	18.0	16.8	—
Average measured over all samplers: 16.9 $\mu g\ m^{-3}$				
Date	Predicted DOE 1	Predicted DOE 2	Predicted DOE 3	Predicted DOE 4
11/8/2018	11.7	11.7	11.8	b
11/9/2018	17.3	16.8	18.2	b
11/10/2018	73.7	40.9	71.9	b
11/11/2018	11.7	11.7	11.7	b
Average	28.6	20.3	28.4	—
Average predicted over all samplers: 25.7 $\mu g\ m^{-3}$				
P/O[a]	1.8	1.1	1.7	—

P/O of sampler average: 1.5

[a] Predicted-to-observed (measured) ratio of sampler time average.

[b] US DOE Sample 4 ceased operation on November 8 and was repaired on December 19, 2018. Because no corresponding measurements existed during the fire, no model predictions were made for DOE-4

[c] Calculated from PM_{10} measurement based on a PM_{10} to $PM_{2.5}$ ratio of 2.05.

that PM_{10} was predicted generally within a factor of 2 of the observations using a similar modeling approach (Grogan et al. 2007). For this study, the average observed value across all samplers was 63.8 $\mu g\ m^{-3}$, the average predicted value was 37.1 $\mu g\ m^{-3}$, and the *P/O* ratio of the averages was 0.58. However, the measured data may include not only $PM_{2.5}$ generated by the Woolsey Fire burning on the SSFL but also $PM_{2.5}$ generated by the Woolsey Fire burning on land outside the SSFL boundary, whereas the modeled concentrations only include $PM_{2.5}$ generated by the Woolsey Fire burning on SSFL land. Consequently, some model underprediction of the measured concentrations in ambient air would be expected.

The distribution of individual *P/O* ratios had an average value of 1.4 (standard deviation 1.90) and a median value of 0.69, suggesting a lognormal distribution. The geometric mean *P/O* ratio was 0.80 and geometric standard deviation was 2.75.

Predicted ambient air concentrations of $PM_{2.5}$ above background are illustrated in Fig. 4. The contours represent the average $PM_{2.5}$ concentration from 8 November 14:00 PST to 10 November 22:00 (57 h). Plumes of $PM_{2.5}$ from areas that burned on 8 November traveled southwest of SSFL and then funneled down a north-south drainage skirting the community of Oak Park. Average concentrations were typically 60 to 90 $\mu g\ m^{-3}$ in this uninhabited region and were lower in the residential areas (20 to 50 $\mu g\ m^{-3}$) of Oak Park and Agoura Hills. A second $PM_{2.5}$ plume from

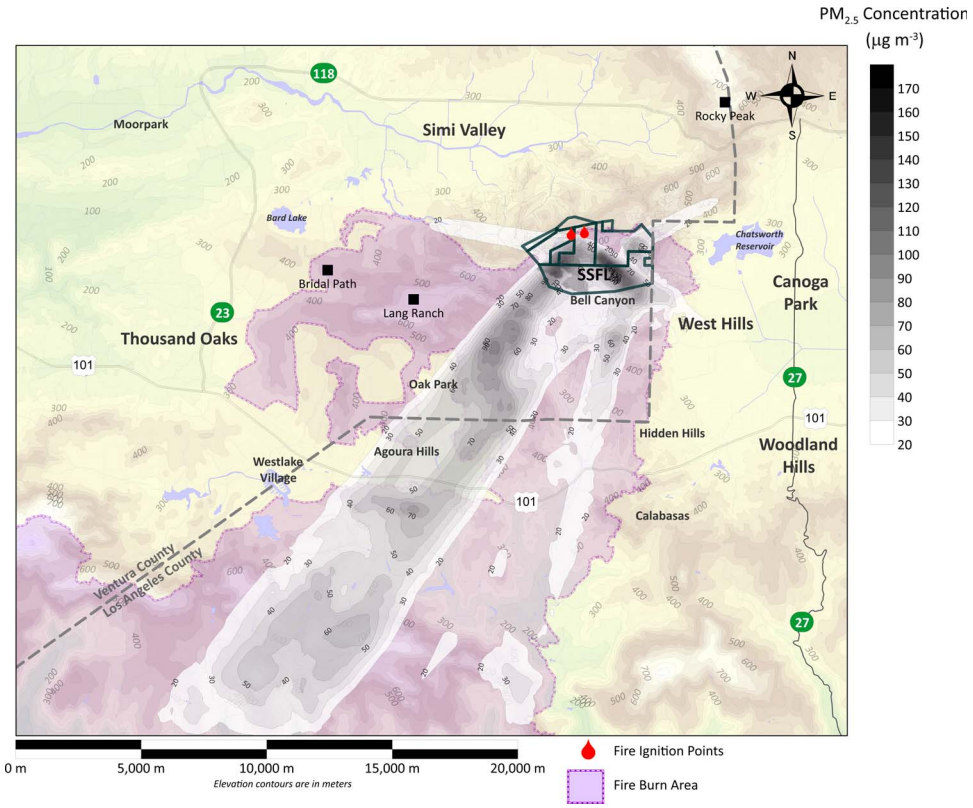

Fig. 4. Isopleth map showing average predicted $PM_{2.5}$ concentration in ambient air from the fire burning across SSFL from 8 November 2018, 14:00 PST to 10 November 2018, 22:00 PST. The entire Woolsey Fire burn area is also shown.

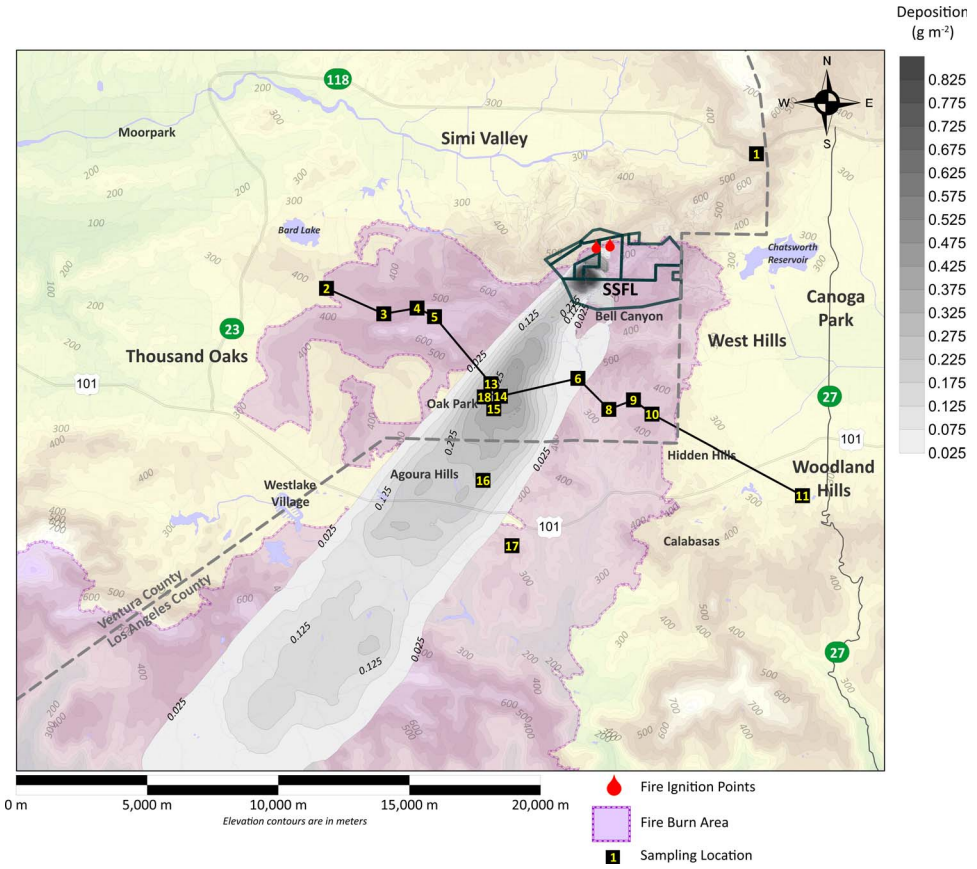

Fig. 5. Isopleth map showing predicted total deposition of particulate matter from Woolsey Fire burning on the SSFL on 8 November in Area IV. The entire Woolsey Fire burn area and soil sampling locations are also shown.

the SSFL Buffer Zone and Area I that burned on 9 and 10 November traveled almost directly south down Bell Canyon at concentrations less than those at Oak Park and Agoura Hills.

Deposition of particulate matter

Airborne particulate matter from burning vegetation and suspended from soil during the fire will eventually deposit on the land surface at a rate based on the dry deposition velocity. For deposition calculations, a particle size distribution larger than $PM_{2.5}$ was assumed (geometric mean of 5 μm, geometric standard deviation of 1.9) so that deposition would include larger particle releases during the fire that were reflected in the PM_{10} and $PM_{2.5}$ air measurements. Larger particles (>10 μm), while not respirable, are subject to gravitational settling and deposit to a greater extent than finer particles. Thus, the magnitude of calculated deposition is lower than probably occurred because the source term was based only on $PM_{2.5}$ emissions. However, what is important is the deposition pattern and the deposition factor (deposition flux divided by release rate). The deposition factor used in later calculations is the deposition rate normalized to the source term and will reflect the deposition of larger particles.

The isopleth map of the predicted deposition across the model domain (Fig. 5) was plotted for releases on 8 November 2018. This deposition pattern is from particulate releases only, while the Woolsey Fire burned in Area IV on the SSFL and does not include deposition from burned areas outside the SSFL boundaries. The highest releases from the Woolsey Fire while burning on the SSFL occurred on 8 November. The deposition pattern generally follows the regional northeast winds at the time of the fire. To the extent any particulate radionuclides on vegetation or in the surface soil from SSFL were potentially suspended during the fire, it would have followed a similar deposition pattern. The highest deposition of particulate matter outside the SSFL boundary was east of the community of Oak Park in a region of hilly uninhabited terrain. Other areas of enhanced deposition correspond to elevated terrain where the lofted plume intersected the ground surface.

During the first day of the Woolsey Fire (8 November), particulate emissions and fire consumption rates on the SSFL were the greatest. The predicted deposition from emissions on 8 November accounted for about 90% of the total deposition in the Oak Park community while the fire burned across the SSFL.

The deposition isopleth map served as a guide for defining a soil sampling program to determine if radionuclides located on the SSFL property and potentially released when the Woolsey Fire burned on the site could be detected at offsite locations. If radionuclides located on the SSFL property were released during the Woolsey Fire, then their presence would most likely be detected in surface soil within the deposition plume from the Woolsey Fire burning on SSFL provided the release quantity was sufficient to result in deposition that could be detected above background.

Radionuclide environmental monitoring data

Measurements of radionuclides in the environment before, during, and following the fire are an important aspect of understanding and quantifying potential impacts from the Woolsey Fire. It is well understood that all wildfires, even in the absence of anthropogenic contamination, release and mobilize radionuclides and other chemicals to the environment (Nance et al. 1993; Lambert et al. 1991; Le Cloarec et al. 1995).

The available air and soil data related to samples collected in the vicinity of the SSFL include routine onsite air and soil sampling of radionuclides performed by US DOE and contractors (Boeing 2005, 2006, 2008) and a soil study conducted by US EPA to estimate background soil concentrations in the vicinity of the SSFL.

US EPA soil background study

The US EPA conducted a study to estimate background concentrations of radionuclides on the SSFL (HydroGeologic 2011). Background included naturally occurring radionuclides and global fallout radionuclides from atmospheric weapons testing. The EPA developed background threshold values (BTVs) for the SSFL region based on samples collected in 2009 at two locations west of the site (Bridal Path and Lang Ranch) and one north of the site (Rocky Peak, see Fig. 1). The EPA considered these locations unimpacted by historical SSFL operations, and additional sampling at distant test locations was done to confirm this. The BTV represents the 95% upper simultaneous limit (USL95) of the distribution of concentrations. The USL95 statistic represents the value such that all observations, not some proportion or percentile, from the established background data set will be less than or equal to USL95 with a confidence coefficient (CC) of 95% (HydroGeologic 2011). The BTVs were determined for 64 radionuclides; however, for this study, only radionuclides considered priority-1 for cleanup activities (HydroGeologic 2012) were considered. Priority-1 radionuclides are those detected on the SSFL by EPA at a concentration that exceeds the radionuclide reference concentration (RRC).

The US EPA background sample locations were selected from within the same two geologic formations exposed on the surface at the SSFL: the Chatsworth and Santa Susana formations. Surface (0-15 cm) and subsurface (>91 cm) samples were collected. A single BTV was estimated for each radionuclide based on a combination of all the data from the different soil horizons and geologic formations that were sampled. However, for fallout radionuclides (^{137}Cs, ^{90}Sr, $^{239/240}$Pu) only the surface sample concentration was used in the background comparison. In general, naturally occurring radionuclide concentrations in the Santa Susana and Chatsworth formations were roughly the same except ^{232}Th, which exhibited higher concentration in the Santa Susana formation (118 Bq kg^{-1}) compared to the Chatsworth formation (85 Bq kg^{-1}). There were also instances of variability within a given formation. For example, ^{226}Ra exhibited higher concentration (58 Bq kg^{-1}) at the Lang Ranch location compared to the Rocky Peak location (43 Bq kg^{-1}), both of which are in the Chatsworth Formation. These background values were used to determine if there was evidence of impact on surface soil samples collected and analyzed as part of this work.

Radionuclide concentrations in soil and vegetation at the SSFL

Extensive soil sampling for radionuclides has been performed in areas of the SSFL with known contamination, and the analytical results for these samples were obtained electronically from Boeing. To estimate an inventory of radionuclides in Area IV soil, statistics were computed for all surface (i.e., top depth of less than 15 cm) soil sample concentrations within Area IV, with no decay correction from the time of sampling and excluding nondetect results and results less than zero. These data are summarized in Table 5 along with their corresponding EPA BTV values from HydroGeologic (2012). Most soil concentration measurements above background at the SSFL occur within Area IV (see Fig. 2) except for ^{226}Ra. Radium-226 concentrations above background (highest concentration of 10 kBq kg^{-1}) remain in the burn pit located in the southwest corner of Area I. The average ^{226}Ra concentration in this region in surface soil was estimated to be 335 Bq kg^{-1} across an area of about 0.009 km^2. The ^{226}Ra surface soil inventory in the burn pit region assuming a surface depth of 3 cm and a bulk density of 1,120 kg m^{-3} was 98.5 MBq. The area of Area I that burned was about 2.22 km^2. Assuming the same bulk density, thickness of a surface layer (3 cm), and a background concentration of ~50 Bq kg^{-1} (lower than the BTV), the ^{226}Ra inventory in Area I surface soil was ~3,750 MBq. Thus, the ^{226}Ra surface soil inventory in the burn pit would represent about 2.6% of the total ^{226}Ra inventory in Area I that burned. Except for ^{60}Co, ^{137}Cs, ^{152}Eu, and ^{90}Sr, the average concentration across all surface soil samples in Area IV was less than the EPA BTV value. The highest individual sample concentration of any radionuclide in soil was for ^{137}Cs (7,252 Bq kg^{-1}). The Woolsey

Table 5. Summary of historical detected radionuclide soil concentrations measured in Area IV of the SSFL and the BTV values. Concentrations include natural background and global fallout and have not been corrected for decay.

Radionuclide	Minimum (Bq kg^{-1})	Maximum (Bq kg^{-1})	Average (Bq kg^{-1})	n	EPA BTV (Bq kg^{-1})	EPA BTV[a] (Bq kg^{-1})
^{60}Co	0.0296	96.2	1.76	108	0.206	0.0717
^{137}Cs	0.0074	7252	22.4	2687	7.14	5.94
^{152}Eu	0.0111	951	12.8	125	0.625	0.412
$^{239/240}$Pu	0.0061	22.7	0.49	663	0.525	0.525
^{226}Ra	7.59	263	42.6	503	69.6	69.3
^{228}Ra[b]	19.98	106	45.5	178	85.1	85.1
^{90}Sr	0.296	1040	19.1	540	2.78	2.29
^{230}Th	2.59	237	33.3	1756	75.5	75.5
^{232}Th	2.33	137	42.7	2326	112	112
^{234}U	8.14	355	32.7	622	69.2	69.2
^{235}U	0.148	27.0	2.3	639	4.81	4.81
^{238}U	3.33	318	31.9	2368	62.2	62.2

[a]The BTV value decay corrected for 8 years (i.e., 2011 to 2019).

[b]Radium-228 is not a priority contaminant as defined in HydroGeologic (2012). The BTV value reported is from HydroGeologic (2011). No decay correction applied because ^{228}Ra would be continuously generated from the decay of ^{232}Th.

Fire burned up to the southern margin of Area IV, but most of the area remained unburned (see Fig. 2).

The surface soil data in Area IV at SSFL were compared to the EPA BTVs (Table 5) to examine the potential for impacts to off-site locations. Plutonium-239, ^{90}Sr, and ^{137}Cs were specifically selected because of their occurrence above background in Area IV and because of the positive detections of ^{239}Pu and ^{90}Sr by Area IV air monitors during the Woolsey Fire (discussed in the next section). Based on the spatial distribution of concentrations, there is a limited area of soil within Area IV where individual sample concentrations of ^{239}Pu, ^{90}Sr, and ^{137}Cs are above background, with most higher concentrations occurring outside of the burned area.

Vegetation was sampled from both on-site and off-site locations during the operational period from 1956 to 1989. Additional vegetation sampling occurred after 1989 during building demolition and site cleanup. Gross alpha and gross beta measurements were reported through 1985 (Moore 1986), and results for specific radionuclides were first reported in 1989 (Moore 1990). Most detected concentrations were for naturally occurring radionuclides (e.g., Rockwell International 1994, Table 5-16). Detections of anthropogenic radionuclides were limited to a measurement of 15 Bq kg^{-1} of ^{60}Co in 1990 (Rockwell International 1991), two detections each of ^{60}Co (maximum = 0.7 Bq kg^{-1}) and ^{137}Cs (maximum = 3.7 Bq kg^{-1}) in 1991 (Rockwell International 1992), a maximum detection of 0.7 Bq kg^{-1} of ^{137}Cs in 1993 (Rockwell International 1994), and a detection of 3.6 Bq kg^{-1} of ^{137}Cs in 1997 (Boeing 1998). The 1989 data are reported on a dry weight basis, and the 2000 results are given on a wet weight basis. Dry or wet weight is not denoted for the detected concentrations in the 1990s. For a given sample, concentrations reported on a dry weight basis will be greater than those reported on a wet weight basis.

A comprehensive vegetation sampling program was conducted in Area IV at the SSFL in 2000 in response to wildfires that had burned on US DOE facilities including Los Alamos National Laboratory, Hanford Nuclear Facility, and Idaho National Laboratory (Boeing 2021). The sampling was conducted in response to public concerns that radionuclides may be emitted to the air from burning vegetation in contaminated areas of SSFL. A composite vegetation sample was taken at each of the 28 legacy radiological facilities in Area IV and two off-site locations. The only radionuclide detected in measurable quantities was naturally occurring ^{40}K with concentrations ranging from the minimum detectable concentration (MDC) (19 Bq kg^{-1}) to 130 Bq kg^{-1}. No anthropogenic radionuclides were detected in either on-site or off-site vegetation. The average MDC for the anthropogenic radionuclides ^{60}Co, ^{137}Cs, and ^{155}Eu were 2 Bq kg^{-1}, 1.7 Bq kg^{-1}, and 2.6 Bq kg^{-1}, respectively.

Activity concentrations in air before, during, and after the Woolsey Fire

Concentrations of gross alpha and gross beta in air were measured before, during, and after the Woolsey Fire by both Boeing (Figs. 6 and 7) and US DOE (Fig. 8). Individual data points are plotted with the 5th and 95th percentile background values estimated using the pre-fire measurement data. Positive detections are identified as results greater than the detection limit and greater than the 2-sigma counting error for the Boeing data, and greater than the detection limit for US DOE data since counter error information was unavailable. Positive detections of gross alpha occurred at both stations for the samples collected

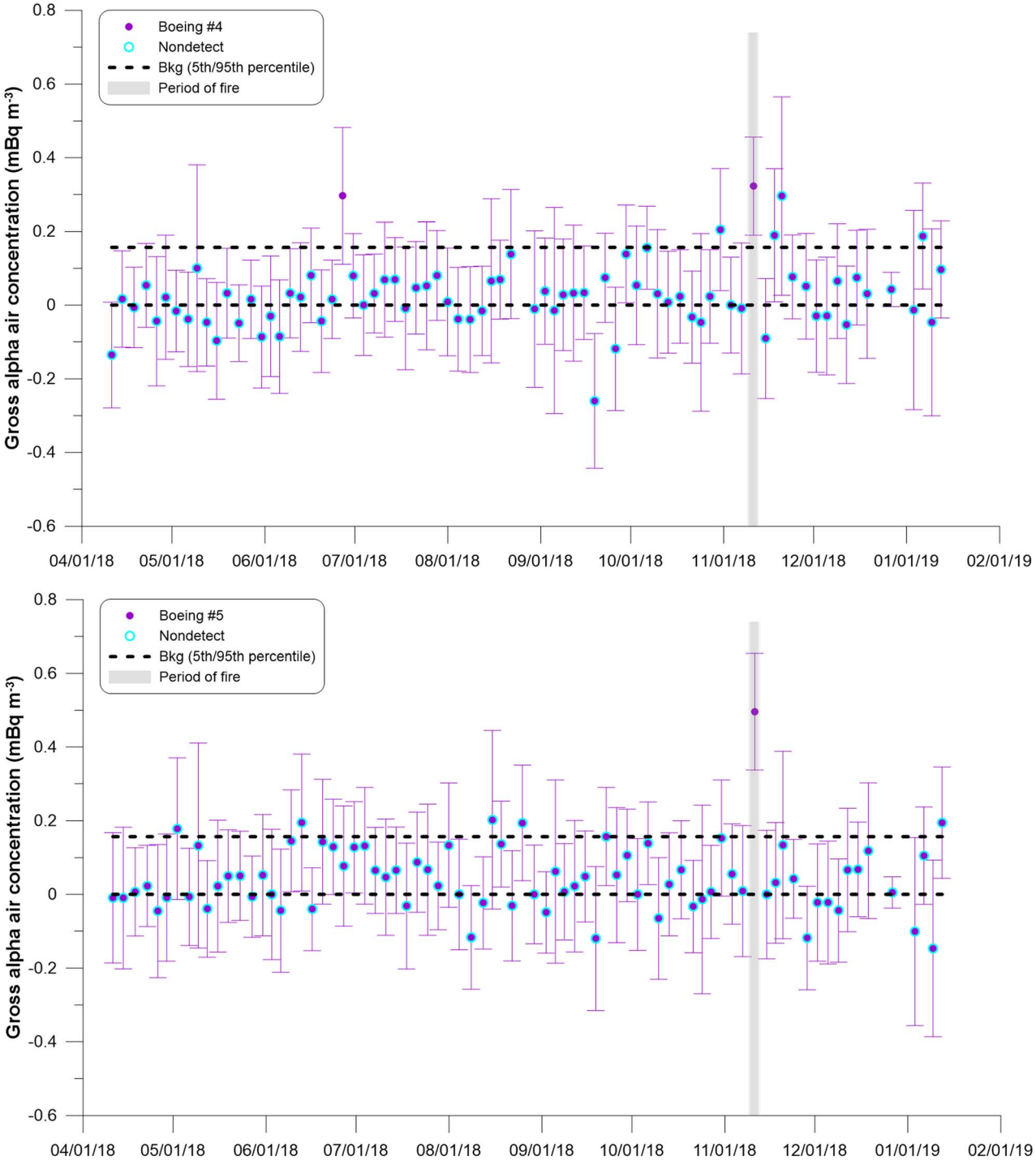

Fig. 6. Gross alpha concentrations in air measured by Boeing at monitoring station 4 and 5. Error bars represent the 2-sigma analytical uncertainty for the measured concentration.

during the fire, as well as one additional sampling period in June 2018 at station 4. The concentration measured during the fire at station 4 is similar to that measured in June 2018 and to levels measured by US DOE at the samplers in Area IV (North Wind 2015, 2018), indicating that the levels of gross alpha measured during the fire were similar to levels measured before the fire. Gross beta concentrations measured at the Boeing stations during the fire were similar to or less than concentrations measured before and after the fire.

Fig. 8 shows gross alpha and beta concentrations in air measured by US DOE at the samplers maintained in Area IV. The samples collected during the fire all had gross alpha concentrations less than the detection limit, although

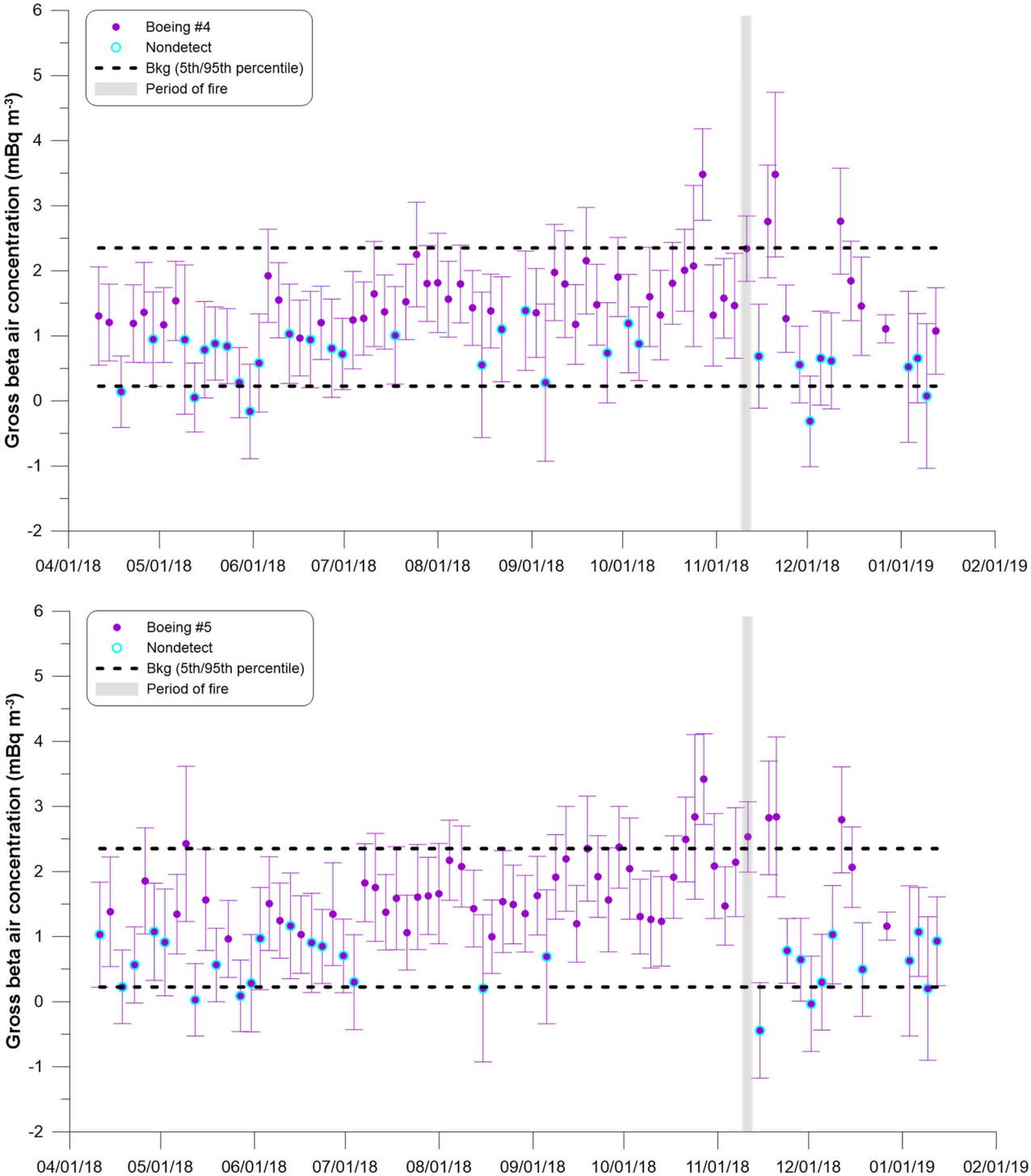

Fig. 7. Gross beta concentrations in air measured by Boeing at monitoring station 4 and 5. Error bars represent the 2-sigma analytical uncertainty for the measured concentration.

concentrations similar to those detected by Boeing at stations 4 and 5 had been detected at the US DOE stations prior to the time of the fire. The gross beta concentration during the fire at DOE-2 had a concentration greater than the detection limit, while the other samplers had concentrations less than the detection limit. Greater gross beta concentrations were measured before the fire at the Area 20 and RMHF stations during the 30 October to 7 November 2018 sampling period and after the fire at the DOE-1 and DOE-2 stations during the 19 to 20 November 2018 sampling period.

Radioisotopic measurements

The air particulate filters collected by Boeing and US DOE during the fire were submitted for isotopic analysis

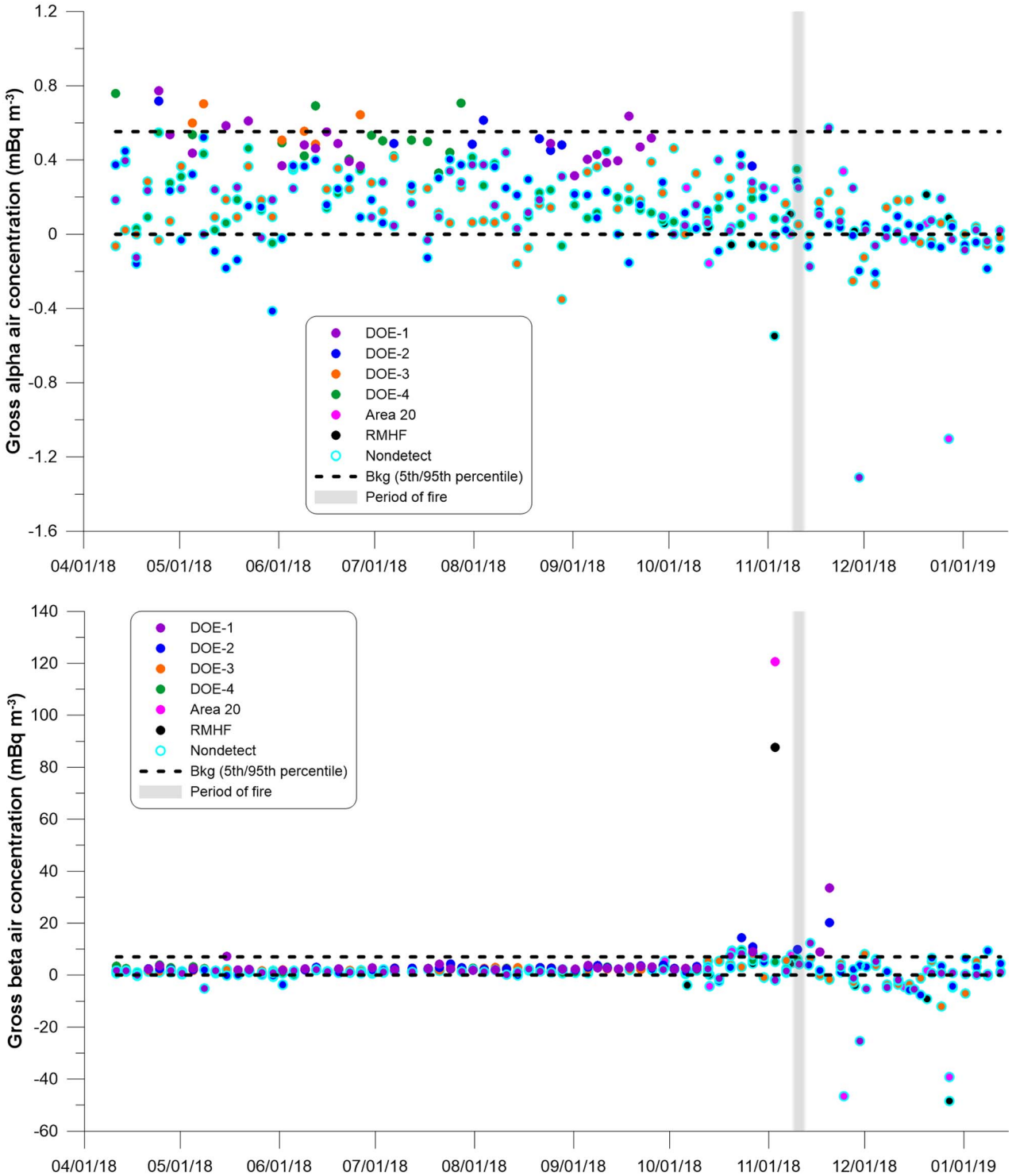

Fig. 8. Gross alpha and beta concentrations in air measured by US DOE in Area IV. Analytical uncertainty was not provided with US DOE sample results.

in addition to the gross alpha and beta measurements discussed above. Positive detections were seen for naturally occurring radionuclides ^{210}Po, ^{230}Th, and ^{232}Th at Boeing stations 4 and 5, which would be expected to be seen for air samples collected during any fire. No anthropogenic radionuclides attributable to SSFL site operations were detected at either station.

The samples from the DOE stations had positive detections for naturally occurring radionuclides ^{228}Ac, ^{228}Ra, ^{226}Ra, ^{230}Th, ^{234}U, ^{238}U, and ^{210}Po, which would be expected

to be detected in samples collected during a fire. There were also detections of ^{239}Pu and ^{90}Sr at the DOE-3 station and of ^{239}Pu at the Area 20 station. Because ^{239}Pu and ^{90}Sr exist in Area IV soils, it is not surprising that concentrations of these nuclides would be detected in the air due to localized resuspension of soil from conditions and activities associated with the fire. Detections of both ^{239}Pu and ^{90}Sr have occurred in the past at Area IV samplers (e.g., Boeing 2005, 2006, 2008; North Wind 2015, 2018), which again is not unexpected due to the proximity of the samplers to soil with elevated concentrations and potential suspension of dust during high wind events.

Plutonium-239 and ^{90}Sr were both detected at Area IV samplers during the fire at concentrations equal to or less than a factor of 2 greater than the detection limit. The concentrations were also approximately an order of magnitude or more below the Derived Concentration Standard (DCS) (US DOE 2021) for both radionuclides (Table 6). The DCS is based on a 1 mSv annual effective dose and assumes continuous exposure at the DCS for 1 y. Therefore, the dose from breathing air with these concentrations during the period of the fire would be significantly less than 0.01 mSv at that location on the SSFL based on the concentrations measured during the fire and the maximum possible exposure duration that could have occurred.

Summary of environmental monitoring data

Several important conclusions can be drawn based on the measurement data. Air samplers operated by Boeing and US DOE and equipped to measure radionuclide concentrations were positioned at various onsite locations in the direction the plume traveled, including areas with soil concentrations above background. Based on measurements made at these locations, the fire had limited impact on gross alpha and beta concentrations measured in air. Some small increases in concentration were seen at the Boeing samplers but at levels similar to concentrations measured at different times before the fire. There was no impact of the fire on gross alpha or gross beta concentrations observed at US DOE samplers (i.e., concentrations measured before the fire are similar to or greater than concentrations measured during the fire). Detection of specific isotopes in air by US DOE samplers in Area IV is likely due to their proximity to soil with concentrations above background in parts of Area IV within the defined fire boundary. Plutonium-239 and ^{90}Sr were the only anthropogenic radionuclides detected by air sampling stations in Area IV. All other detections in Area IV were for naturally occurring radionuclides. The concentrations of ^{239}Pu and ^{90}Sr detected in air in Area IV were well below concentration standards defined for human health protection that assume continuous exposure for 1 y, and any exposures at the SSFL site boundary associated with the Woolsey Fire would be of short duration occurring only during the fire. The Boeing air stations in Area I did not detect SSFL-related anthropogenic radionuclides, nor did the other four US DOE Area IV air samplers, indicating that the slightly elevated air concentrations were limited to the immediate vicinity of Area IV with soil concentrations above background. Historical monitoring of vegetation resulted in a few sporadic detections of ^{137}Cs and ^{60}Co, and a comprehensive vegetation survey in 2000 did not detect any anthropogenic radionuclides in either onsite or offsite vegetation.

Potential release quantities, hypothetical effective dose, and minimum detectable dose from deposition

This section evaluates the potential inventory of radionuclides in soil on the SSFL and the likelihood of detecting these radionuclides in soil in the Oak Park community if this inventory was released and migrated offsite during the Woolsey Fire. The Oak Park community is located about 6 km southwest of the SSFL and was the region of highest predicted offsite deposition of particulate matter. A second evaluation calculates the minimum detectable dose from confirmatory soil sampling described in a later section for samples taken in Oak Park. Both calculations rely on the concentration and deposition factors determined with CALPUFF for burn areas 1 through 5 and integrated over a 10-hour period, which corresponds to the specific regions and timing of when the fire burned in the area where most of the radionuclide inventory in soil exists. Concentration and deposition factors are given by

$$X/Q = \frac{X_{air}}{Q}, \qquad \psi/Q = \frac{\psi_{grd}}{Q}, \tag{1}$$

where

X_{air} = 10-h average $PM_{2.5}$ concentration (2.93×10^{-4} g m^{-3});

Table 6. Concentrations (mBq m^{-3}) of ^{239}Pu and ^{90}Sr measured in air by US DOE samplers in Area IV.

Station	Nuclide	Air concentration	Detection limit	Solubility class	DCS[a]	% of DCS
DOE-3	^{239}Pu	0.107	0.09	M	5.4	1.98%
	^{90}Sr	1.27	0.847	M	4100	0.03%
Area 20	^{239}Pu	0.323	0.323	M	5.4	5.98%

[a]Source: US DOE (2021).

ψ_{grd} = 10-h average deposition rate on the ground surface (8.9×10^{-6} g m^{-2} s^{-1});

Q = release rate of $PM_{2.5}$ during the 10-hour simulated time period (8,300 g s^{-1});

X/Q = concentration factor for Oak Park (3.53×10^{-8} s m^{-3}); and

ψ/Q = deposition factor (1.07×10^{-9} m^{-2}).

The X/Q and ψ/Q values were based on a $PM_{2.5}$ emission rate. As noted earlier, deposition calculations assumed a larger particle size distribution to account for greater deposition of larger particles. The calculations focused on three anthropogenic radionuclides that have been detected in soils on the SSFL: ^{137}Cs, ^{90}Sr, and ^{239}Pu, and the naturally occurring radionuclide ^{234}U. Uranium-234 was chosen because it had the highest concentration of a naturally occurring radionuclide in Area IV surface soil and was identified as a priority-1 radionuclide for cleanup activities.

A bounding estimate of the maximum potential radionuclide releases from the Woolsey Fire burning on the SSFL is to assume the radionuclide inventory in the top 3 cm of Area IV soil, including background, was released to the air as small particulates. This entire inventory is assumed to be within fire burn areas 1 through 5 (see Fig. 2) which include the portion of Area IV that burned. Burn area 5 is included because this area burned during the evening of 8 November 2018 and is included in the dispersion and deposition factor estimates. Assuming the upper 3 cm of soil is released from the site (a bounding assumption) the areal concentration is given by

$$C = (C_{soil} \times \rho_b \times T \times A) \times \frac{\psi}{Q}, \qquad (2)$$

where

C = areal concentration from deposition on soil surface at Oak Park (Bq m^{-2});

C_{soil} = average soil concentration in Area IV of SSFL (see Table 5, Bq kg^{-1});

ρ_b = bulk density (1.12×10^3 kg m^{-3});

T = layer thickness at SSFL (0.03 m);

ψ/Q = deposition factor for Oak Park (1.07×10^{-9} m^{-2} from CALPUFF modeling); and

A = area of fire regions 1–5 (30,521,141 m^2).

Measured bulk densities in the 0-3 cm layer from sampling described in the later section on confirmatory soil sampling ranged from 0.76 g cm^{-3} to 1.49 g cm^{-3} with a mean of 1.12 g cm^{-3}. The concentration (Bq kg^{-1}) in surface soil at Oak Park is the areal concentration divided by the product of the bulk density (also assumed to be 1,120 kg m^{-3}) and the surface sampling thickness (3 cm). The predicted hypothetical concentration of ^{137}Cs, ^{90}Sr, ^{239}Pu, and ^{234}U in the 0–3 cm soil layer in Oak Park calculated using eqn (2) is both below typical detection limits (~0.4 Bq kg^{-1} for ^{137}Cs and ^{90} Sr, to ~0.8 Bq kg^{-1} for Pu and U isotopes) and would be impossible to distinguish from background (Table 7). Eqn (2) does not correct for background and thus overestimates the actual SSFL-derived radionuclide inventory in onsite soil. The results from applying eqn (2) demonstrate that the radionuclide inventory present on the SSFL is insufficient to produce a measurable impact in bulk off-site soils. It might be argued that radionuclides deposited would concentrate in the fines (silt and clay-sized particles, <4 μm diameter). If this were the case, then concentrations would be higher and might be detected. For example, suppose the soil is defined as a sandy clay loam with a clay mass fraction of 27.4% (Carsel and Parrish 1988) and all the activity deposited was concentrated in the clay particles, the mass which contains the radionuclides would be only 27.4% of the bulk mass and concentrations would increase by a factor of 1/0.274 = 3.65. Even if this were the case, concentrations would still either be below detection limits or indistinguishable from background.

A similar calculation can be made assuming the ^{137}Cs concentration in vegetation in burn areas 1 through 5 is at the MDC value of 1.72 Bq kg^{-1} wet weight with a total wet weight biomass of 4.26 kg m^{-2} calculated from the fuel loads. The hypothetical inventory of ^{137}Cs in vegetation that would be released assuming a concentration of 1.72 Bq kg^{-1} wet weight is 22.6 MBq. This is a factor of 100 less than the soil release inventory given in Table 7. The hypothetical deposition amounts based on vegetation burning would also

Table 7. Bounding estimate of the radionuclide inventory in the 0–3 cm layer on the SSFL, predicted deposition and soil concentration at Oak Park, and comparison to decay-corrected background BTV.

Radionuclide	Average SSFL soil concentration (Bq kg^{-1})	Average SSFL soil concentration (Bq m^{-2})[a]	Bounding inventory released from SSFL (MBq)	Predicted deposition at Oak Park (Bq m^{-2})	0–3 cm concentration at Oak Park (Bq kg^{-1})	Background BTV (Bq kg^{-1})[b]
^{137}Cs	22.4	753	2,297	2.46	0.07	5.94
^{239}Pu	0.490	16	50.3	0.054	0.0016	0.525
^{90}Sr	19.1	642	1,959	2.10	0.06	2.29
^{234}U	32.7	1099	3,353	3.59	0.11	62.9

[a]Calculated assuming a soil depth of 0.03 m and a bulk density of 1,120 kg m^{-3}.

[b]The BTV value decay corrected for 8 years (i.e., 2011 to 2019).

be a factor of 100 less than the soil values in Table 7 and would therefore not contribute significantly to the soil deposition concentrations.

A second calculation was performed to determine the minimum detectable dose above background that could be estimated due to hypothetical deposition from the Woolsey Fire burning across the SSFL using the soil profile sampling in Oak Park. For this calculation, a detectable amount was assumed to be 25% of the decay corrected BTV value above background. The 25% BTV value was based on (1) variability of radionuclide concentrations measured in surface soils and (2) analytical uncertainty in the measurements. Based on the confirmatory soil sampling discussed later, surface soil samples (0–3 cm depth) in the Oak Park region had a coefficient of variation ranging from 10.3% for ^{137}Cs to 18.5% for ^{234}U. Strontium-90 and ^{239}Pu were not detected in any of those samples. Analytical measurements had an average coefficient of variation ranging from 13% for ^{234}U to 15.2% for ^{137}Cs. Thus, it is reasonable to assume that a surface soil measurement that is 25% of the BTV above background in the surface soil could be attributable to a deposition event and distinguishable from natural variability or analytical uncertainty. The hypothetical exposure scenario considered inhalation and submersion during plume passage, external exposure from radionuclides deposited in the soil, and inhalation of resuspended radionuclides deposited in soil. The minimum detectable effective dose (D_{md}) was calculated by

$$D_{md} = Q\left[\begin{array}{l}\left(X/Q \times BR_F \times DC_{inh} \times \frac{\text{hr}}{3600\ \text{s}}\right) + (X/Q \times DC_{sub}) + \\ \left(\psi/Q \times ET_{grd} \times \frac{3600\ \text{s}}{\text{hour}} \times DC_{grd}\right) + (\psi/Q \times BR_A \times ET_{res} \times RF \times DC_{inh})\end{array}\right], \quad (3)$$

where

Q = radionuclide source that would correspond to deposition in Oak Park of 25% of the BTV value when mixed in the top 3 cm of soil (Bq);

BR_F = breathing rate during fire (0.945 m^3 h^{-1});

BR_A = breathing rate after fire (0.67 m^3 h^{-1});

DC_{inh} = dose coefficient for inhalation (Sv Bq^{-1});

DC_{sub} = submersion dose coefficient (Sv m^3 s^{-1} Bq^{-1});

DC_{grd} = ground plane dose coefficient (Sv m^2 s^{-1} Bq^{-1});

ET_{grd} = external exposure time for radionuclides deposited on the ground (5,256 h);

ET_{res} = exposure time for radionuclides deposited on the ground that are resuspended (6,570 h);

RF = resuspension factor (2.0 × 10^{-6} m^{-1});

X/Q = concentration factor for Oak Park (3.53 × 10^{-8} s m^{-3}); and

ψ/Q = deposition factor for Oak Park (1.07 × 10^{-9} m^{-2}).

The Q value that corresponds to a deposition amount of 25% of the BTV is calculated using

$$Q = \frac{C_{25} \times \rho_b \times T}{\psi/Q}, \quad (4)$$

where

ρ_b = bulk density (1,120 kg m^{-3});

T = thickness of soil layer (0.03 m); and

C_{25} = 25% of the BTV value (Bq kg^{-1}).

The hypothetical exposure scenario assumes that while the fire burned across the SSFL, the person is engaged in light activity 75% of the time and moderate activity for the remainder (Table 8). Mean breathing rates for light and moderate activity for a person 31 to 41 years old are 0.012 m^3 min^{-1} (0.72 m^3 h^{-1}) and 0.027 m^3 min^{-1} (1.62 m^3 h^{-1}), respectively (US EPA 2019), for a weighted mean of 0.945 m^3 h^{-1} during the fire. After the fire and for the remainder of the year, the annual mean inhalation rate of 0.67 m^3 h^{-1} is assumed and default occupancy factors from RESRAD v7.2 (Kamboj et al. 2018) were used. These factors include 50% of the time spent indoors, 25% of the time spent outdoors, 25% of the time spent away from the home, and an indoor gamma shielding factor of 0.7. The occupancy factor multiplied by the number of hours in a year (8,760) gives the hypothetical exposure time from external exposure for radionuclides deposited on the ground. The occupancy factor (OF) and exposure time for ground exposure (EF_{grd}) is calculated as

$$OF = 0.5 \times 0.7 + 0.25 \times 1.0 + 0.25 \times 0.0 = 0.6$$

$$ET_{grd} = 0.6 \times 8{,}760\ \text{h} = 5{,}256\ \text{h}$$

The exposure time for inhalation of deposited radionuclides that have been resuspended (EF_{res}) is the total hours in a year (8,760) times fraction of time spent at home (0.75).

The resuspension factor is initially ~10^{-5} m^{-1}, which decays with a halftime of ~50 days to ~10^{-9} m^{-1} over the long term due to weathering and other physical processes (Whicker and Rood 2008). For these calculations, the resuspension factor is integrated and averaged over a year to yield a value of 2 × 10^{-6} m^{-1}.

Dose coefficients, shown in Table 9, are from US DOE (2021) for inhalation and from US EPA (2019) for external exposure (submersion and ground plane) and represent the latest internal and external dosimetry. The inhalation dose coefficients are based on a 1-μm aerodynamic equivalent diameter.

The calculated hypothetical minimum detectable doses (Table 10) ranged from 6.8 × 10^{-5} mSv for ^{90}Sr to 0.024 mSv for ^{234}U. The ^{234}U minimum detectable dose is substantially higher than the other radionuclides because the background concentration of ^{234}U is much higher. The minimum detectable doses are substantially below the annual effective dose limit above background from human sources recommended by the International Commission on Radiological Protection (ICRP), the National Council on Radiation

Table 8. Exposure scenario parameters used in the dose calculation.

Parameter	Value	Units	Reference or comments
Breathing rate during fire, BR_F	0.945	$m^3\ h^{-1}$	Calculated from data in US EPA (2019)
Breathing rate remainder of the year, BR_A	0.66	$m^3\ h^{-1}$	US EPA (2019) mean value
Occupancy factor, *OF*	0.6	—	Calculated based on Kamboj et al. (2018)
Exposure time for resuspension	6,570	hours	Assumes 75% of time spent at home
External exposure time, ET_{grd}	5256	hours	Calculated based on Kamboj et al. (2018)
Resuspension Factor, *RF*	2×10^{-6}	m^{-1}	Integrated value based on Whicker and Rood (2008)
Soil layer thickness, *T*	0.03	m	Sampling depth for surface soil

Protection and Measurements (NCRP), and implemented in DOE-Order 458.1 (US DOE 2020) of 1 mSv y^{-1}. The calculated minimum detectable doses are also well below the average effective dose from natural background a typical person normally receives in a year of about 3.1 mSv (NCRP 2009). Thus, the confirmatory soil sampling discussed later can detect doses from potential deposition from the Woolsey Fire that are substantially less than regulatory limits or doses from natural background. Moreover, the release that would correspond to those dose detection limits is much greater than the bounding estimate of the inventory currently present in soil on the SSFL. As discussed earlier, even if the entire inventory in Table 7 were released, the total hypothetical dose using the previously described exposure model would be less than 0.0002 mSv.

These calculations demonstrate that:

1. The surface soil activity inventory in Area IV of the SSFL if released during the Woolsey Fire and migrated offsite is insufficient to result in a detection in surface soil in the region of highest offsite deposition (Oak Park);
2. Even if this inventory had been released and migrated offsite, the resulting annual effective dose would be less than 0.0002 mSv to a person in Oak Park; and
3. The confirmatory soil sampling method discussed in the next section is capable of detecting an annual effective dose from deposition that ranges from 6.8×10^{-5} mSv for ^{90}Sr to 0.024 mSv for ^{234}U. These doses are well below regulatory standards and natural background.

Confirmatory soil sampling

Soil sampling was used to confirm the conclusions reached in the previous section. That is, any radionuclide release from SSFL sources during the fire and subsequent deposition on soil would not be discernable from background. Sampling locations were selected to include three distinct areas:

- Areas where potential deposition of any radionuclides from the Woolsey Fire burning on the SSFL would have been most likely to occur;
- Areas on either side of the particulate deposition plume from the fire; and
- Areas upwind during the fire that would be unaffected. These samples were obtained to characterize background concentrations of radionuclides.

A reconnaissance trip taken 4 and 5 June 2019, identified potential sampling locations based on their proximity

Table 9. Dose coefficients (DC) used in dose calculation.

Radio-nuclide	Progeny[a]	Inhalation solubility Type[b]	Inhalation DC (Sv Bq^{-1})	Ground plane DC (Sv-m^2 Bq^{-1} s^{-1})	Submersion in air DC (Sv-m^3 Bq^{-1} s^{-1})
^{137}Cs[c]		M	8.73×10^{-9}	7.85×10^{-18}	3.89×10^{-16}
	^{137m}Ba	M	[e]	3.90×10^{-16}	2.66×10^{-14}
^{239}Pu		M	2.74×10^{-5}	4.18×10^{-20}	3.30×10^{-18}
^{90}Sr[d]		M	3.64×10^{-8}	6.52×10^{-18}	4.03×10^{-16}
	^{90}Y	M	[e]	4.17×10^{-16}	3.18×10^{-15}
^{234}U		M	2.40×10^{-6}	6.42×10^{-20}	5.15×10^{-18}

[a]Radioactive progeny that are in secular equilibrium in the environment.

[b]Default solubility class as reported in Table 5 of US DOE (2021). Inhalation DCs are based on a 1 μm aerodynamic equivalent diameter.

[c]External doses for ^{137}Cs includes the dose from ^{137}Cs plus the dose from ^{137m}Ba × the branching fraction of 0.944.

[d]External doses for ^{90}Sr includes the dose from ^{90}Sr plus the dose from ^{90}Y × the branching fraction of 1.0.

[e]Inhalation dose coefficient includes these progenies.

Table 10. Estimated minimum detectable annual effective dose in surface soil from atmospheric transport and deposition in Oak Park from the Woolsey Fire.

	Minimum detectable effective doses by pathway (mSv)					
Radionuclide	Inhalation[a]	Submersion[a]	External	Resuspension	All pathways	Required release (MBq)[b]
^{137}Cs	3.8×10^{-6}	4.2×10^{-8}	3.6×10^{-4}	3.8×10^{-6}	3.6×10^{-4}	46,560
^{239}Pu	1.0×10^{-3}	4.8×10^{-13}	3.5×10^{-9}	1.1×10^{-3}	2.1×10^{-3}	4,115
^{90}Sr	6.1×10^{-6}	2.3×10^{-9}	5.6×10^{-5}	6.1×10^{-6}	6.8×10^{-5}	17,950
^{234}U	1.2×10^{-2}	9.9×10^{-11}	7.1×10^{-7}	1.2×10^{-2}	2.4×10^{-2}	542,414

[a]Effective doses incurred during plume passage.

[b]The activity required to be released from SSFL that would result in a 0–3 cm soil concentration in Oak Park that is 25% of the decay-corrected BTV above background.

to the particulate deposition plume and accessibility. Permissions were obtained for 16 sample locations, and those locations were sampled in August 2019 (see Fig. 5). Sampling was concentrated in the region of highest estimated particulate deposition (locations 13, 14, 15, 16, and 18) off the SSFL property. None of the locations are impacted by surface water that drains from SSFL.

Sample locations and geology

Sample location coordinates and associated geologic formation information are summarized in Table 11 and plotted in Fig. 9 along with a simplified geologic map adapted from Yerks and Campbell (2005). Additional sampling location details are provided in Rood et al. (2020). The local geology is important because naturally occurring radionuclides vary in abundance depending on the source rock. Naturally occurring radionuclides include those that are part of the uranium and thorium decay series, and potassium-40. The US EPA background study (HydroGeologic 2011) focused on samples taken from the same geologic formations that are exposed on the SSFL because they reflect the same natural abundance of naturally occurring radionuclides. US EPA background samples at Lang Ranch (near location 5) and Rocky Peak (near location 1) were taken from the Chatsworth formation. Background samples identified as Bridal Path (near location 2) were taken in the Santa Susana formation. For some radionuclides, notably ^{232}Th, US EPA noted higher concentrations in the Santa Susana formation compared to the Chatsworth formation. According to the US EPA background study, about 80% of Area IV is underlain by the Chatsworth formation and the remainder is underlain by the Santa Susana formation. Most of the SSFL site, including the buffer areas, is underlain by the Chatsworth formation.

The oldest formation in the study area was the Cretaceous-age Chatsworth formation, which is composed

Table 11. Sample location coordinates and geologic formation.

Location number [a]	Latitude (dd)[b]	Longitude (dd)[b]	UTM E (m)[c]	UTM N (m)[c]	Geologic formation
1	34.2681	118.6373	349268	3793094	Chatsworth formation
2	34.2193	118.8143	332872	3787960	Santa Susana formation
3	34.2109	118.7904	335057	3786985	Chatsworth formation
4	34.2131	118.7767	336326	3787207	Chatsworth formation
5	34.2102	118.7694	336992	3786880	Chatsworth formation
6	34.1898	118.7097	342461	3784525	Calabasas formation & Alluvium
8	34.1793	118.6967	343640	3783338	Modelo formation
9	34.1827	118.6565	344579	3783702	Modelo formation
10	34.1779	118.6788	345286	3783159	Towsley formation
11	34.1508	118.6160	351021	3780058	Modelo – sandstone/diatomaceous member
13	34.1875	118.7456	339145	3784317	Calabasas/Modelo formation & Alluvium
14	34.1832	118.7416	339504	3783843	Modelo formation
15	34.1789	118.7442	339252	3783363	Modelo formation &Alluvium
16	34.1543	118.7482	338842	3780645	Modelo/Calabasas formation
17	34.1319	118.7358	339945	3778145	Calabasas formation
18	34.1829	118.7483	338888	3783814	Modelo formation

[a]Location 7 was deleted because of its proximity to location 6. Location 12 was deleted because permission was not received from the property owner to take a sample.

[b]Decimal degrees.

[c]Universal Transverse Mercator East, Zone 11, North American Datum 83.

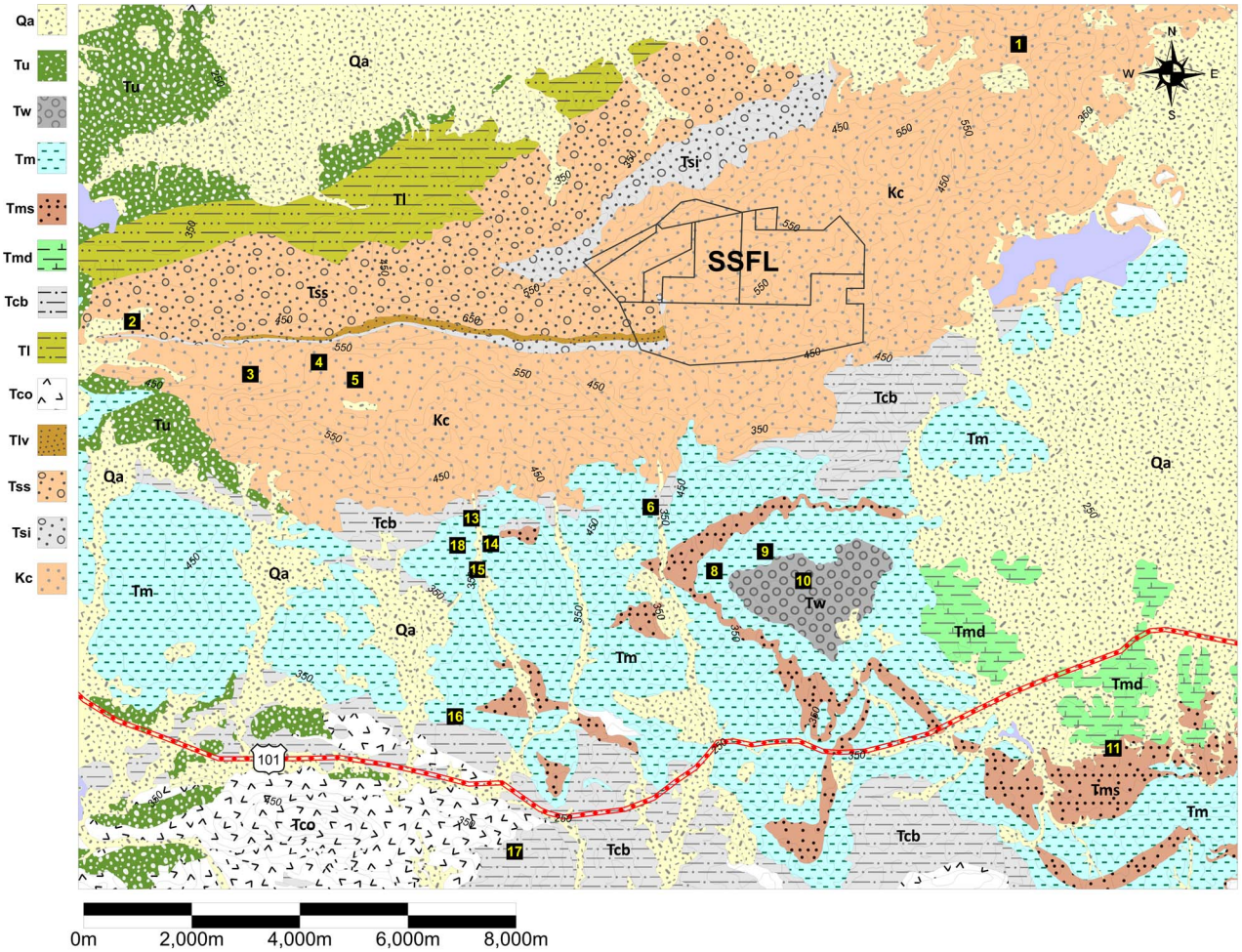

Qa Quaternary alluvium, undivided: Tu Tertiary sedimentary deposits, undivided: Tw Towsley formation, undivided: Tm Modelo formation, undivided: Tms Modelo formation, sandstone: Tmd Modelo formation, diatomaceous shale: Tcb Calabasas formation, undivided: Tl Llajas formation: Tco Conejo Volcanics, undivided: Tss Santa Susana formation: Tsi Simi conglomerate: Kc Chatsworth formation

Fig. 9. Simplified geologic map of the study area showing the SSFL and soil sampling locations. Faults, folds, and other structural features are not shown (adapted from the GIS files provided in a supplement to Yerks and Campbell 2005).

of massive, thick-bedded medium- to coarse-grained turbidite sandstone and well cemented conglomerate (Yerks and Campbell 2005). The conglomerate contains rounded clasts of porphyry and granitic rocks. The overlying early Eocene to late Paleocene-age Santa Susana formation consists of clay, shale, and fractured mud stone interbedded with fine- to medium-grained sandstone and pebble conglomerate. There are also lenses of gray limestone concretions that are common in shale. Sample location 2 was in the Santa Susana formation, and samples 1, 3, 4, and 5 were in the Chatsworth formation. The Miocene-age Calabasas formation underlays sample locations 6, 13 and 17, but location 6 and 13 are also near the contact with Quaternary alluvium deposits and the Modelo formation. Depth profiles of ^{137}Cs and proximity to the drainage bottom suggest these locations have been reworked by fluvial processes. The late Miocene Modelo formation underlays samples 8, 9, 11, 14, 15, 16, 18. Sample location 10 is underlain by the early Pliocene/late Miocene age Towsley formation, which overlies and interfingers with the Modelo formation in the Santa Susana Mountains. The Calabasas formation consists of interbedded clayey to silty sandstone and silty shale with local beds of sedimentary breccia. The Modelo formation lies unconformable above the Calabasas formation and consists of gray to brown, thin-bedded mudstone shale or siltstone with interbeds of very fine- to coarse-grained sandstone. Samples 8 and 9 lie within a subdivision of the Modelo consisting primarily of sandstone, and sample 11 lies on the contact of a sandstone and diatomaceous shale subdivision of the Modelo formation. The Towsley formation is the youngest formation and consists of interbedded sandstone, mudstone, and conglomerate.

Sampling protocol

The soil sampling protocol was adapted from the protocol used by Webb et al. (1997) and Rood et al. (2008) to detect plutonium and uranium deposition from atmospheric plumes. The protocol uses depth profiles to determine

activity levels in layers starting from the surface and extending to depth. Webb et al. (1997) and Rood et al. (2008) demonstrated that most radionuclide deposition (>80%) that occurred 30 to 60 y ago remains in the top 6 cm of soil. Less than a year elapsed between potential deposition and the sampling in the case of the Woolsey Fire. Therefore, the activity contained within each layer provides evidence of the source because if activity were deposited from the atmosphere recently, most of the activity will reside in the first layer. This sampling strategy assumes that the soil has remained relatively undisturbed from the time of deposition which was visually verified during sampling.

Samples were taken at locations undisturbed since the fire with no obvious evidence of surface runoff, erosion, or soil accumulation. Cesium-137 is often used to determine soil disturbance because above-ground nuclear weapons testing resulted in worldwide deposition of ^{137}Cs in measurable quantities on soils. Most of the cesium remains in the surface layer because it is relatively immobile due to its comparatively high soil-water partitioning coefficient. Thus, a depth profile that shows most of the ^{137}Cs activity in the surface layer would indicate the soil has been undisturbed since global fallout. In this case, soil only needs to be undisturbed since the Woolsey Fire to determine if higher concentrations exist in the surface layer. Cesium-137 has also been detected in SSFL soils and thus may have potentially been emitted during the fire. If ^{137}Cs were emitted from the SSFL during the Woolsey Fire and deposited at downwind locations, then the surface soil concentration would be statistically greater than that associated with global fallout, the concentration of ^{137}Cs in the surface soil would have to be higher than in the subsurface layers, *and* the sample would have to have been taken within the Woolsey Fire deposition plume.

Sampling procedure

Sample locations (Fig. 5) were numbered from 1 to 18 with locations 7 and 12 subsequently omitted because either they were too close to other locations or permission could not be obtained. Samples were identified by the sample location number followed by a depth designation letter (A = 0–3 cm, B = 3–6 cm, C = 6–12 cm). Duplicate samples had "-D" after the depth designation letter. One sample was split (sent to a different laboratory) and identified by "-S" following the depth designation letter.

Hand tools were used to excavate a 25 cm × 25 cm area for three depth horizons: 0-3 cm, 3-6 cm, and 6-12 cm (Fig. 10). The area was cut in half for the 6-12 cm so that the same volume of sample was obtained for each layer (~1.875 L). Hand tools were cleaned between sampling each layer. A Ludlum Model 3 rate meter with a detached 2.5 in × 2.5 in NaI(Tl) probe was used to characterize the gamma exposure rate at each sampling site.

Analytes and laboratory analysis

Samples were sent to GEL Laboratories, LLC (GEL), and one sample split was sent to TestAmerica, Inc. Chain-of-custody forms accompanied each shipment of samples. Radionuclides for which analysis was requested included all the radionuclides reported in the EPA background study (HydroGeologic 2011), except for ^{113m}Cd, ^{222}Rn, and ^{220}Rn. GEL does not analyze for ^{113m}Cd because the analytical methods are incapable of detecting this radionuclide at concentrations that could conceivably be in soil. The ^{113m}Cd MDC in the US EPA background study was 74,000 Bq kg^{-1}. The radon isotopes were short half-life noble gases that are the progeny of ^{224}Ra and ^{226}Ra, respectively, and would not be present without the presence of their parent. Results were provided for 61 radionuclides. This paper focuses on the priority-1 radionuclides that were detected above the radiological reference concentrations (RRC) in the US EPA Area IV Radiological Study. Complete results for all 61 radionuclides are presented in Rood et al. (2020).

RESULTS

Sample results for priority-1 radionuclides that had two or more detections (above the minimum detectable concentration) in the three soil layers at each sampling location are summarized in Table 12. A complete tabulation of results is presented in Rood et al. (2020). Priority-1 radionuclides that had two or more detections at each location were limited to uranium decay series radionuclides (^{238}U, $^{233/234}$U, ^{230}Th, and ^{226}Ra) and ^{137}Cs. A depth weighted-average concentration was computed for comparison to the BTV value because the BTV value is based on a 15-cm-thick soil sample. The depth weighted-average concentration is given by

$$C_{wt} = \frac{C_3 \times 3\text{ cm} + C_6 \times 3\text{ cm} + C_{12} \times 6\text{ cm}}{12\text{ cm}}, \quad (5)$$

where

C_3 = radionuclide soil concentration in 0–3 cm layer (Bq kg^{-1});

C_6 = radionuclide soil concentration in 3–6 cm layer (Bq kg^{-1}); and

C_{12} = radionuclide soil concentration in 6–12 cm layer (Bq kg^{-1}).

Analytical uncertainty was propagated through to the weighted average concentration using (Bevington and Robinson 1992)

$$\sigma_w = \sqrt{\frac{a^2\sigma_a^2 + b^2\sigma_b^2 + c^2\sigma_c^2}{(a+b+c)^2}}, \quad (6)$$

where

σ_w = standard deviation of weighted mean concentration (Bq kg^{-1});

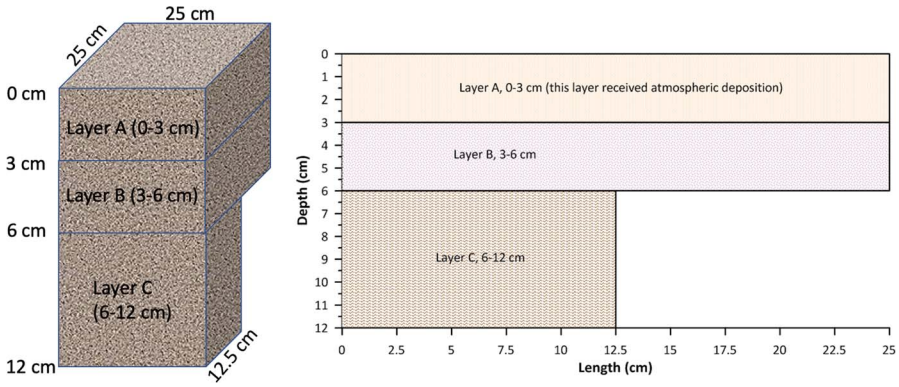

Fig. 10. Depth profile sampling layers. Each layer contained 1,875 cm^3 of soil. The area of the lowest sampled layer (6–12 cm) was halved to 25 cm × 12.5 cm. The 0- to 3-cm top layer would contain atmospheric deposition from the Woolsey Fire and ^{137}Cs from global fallout.

σ_a = analytical uncertainty in the 0–3 cm layer (Bq kg^{-1});
σ_b = analytical uncertainty in the 3–6 cm layer (Bq kg^{-1});
σ_c = analytical uncertainty in the 6–12 cm layer (Bq kg^{-1}); and
a, b, c = 3 cm, 3 cm, and 6 cm, respectively.

A one-tailed t-test was performed to test whether the depth-weighted average concentration was greater than the BTV value (α = 0.025, $df = \infty$, t = 1.98). Thus, the null and alternative hypothesis and calculated t value are

$$\begin{aligned} H_o &: \overline{X} \leq BTV \\ H_a &: \overline{X} > BTV \\ t &= \frac{\overline{X} - BTV}{\sigma} \end{aligned}, \qquad (7)$$

where $\overline{X}$ is the weighted average concentration, C_{wt}.

Exceedances of the BTV value were observed for ^{226}Ra at locations 8, 11, and 13; ^{230}Th at location 11; $^{233/234}U$ at location 11; and ^{238}U at locations 8 and 11. There were no exceedances of anthropogenic radionuclides (e.g., ^{137}Cs, ^{90}Sr, ^{239}Pu, etc.). Location 13 is in the location of highest deposition, while locations 8 and 11 lie east of location 13 and outside the region of deposition. All BTV exceedances occurred in locations of different geologic formations than those sampled in the EPA background study. The highest concentrations of uranium series radionuclides (^{238}U, ^{234}U, ^{230}Th, and ^{226}Ra) were observed at location 11, which was most distant from the fire and well outside the deposition plume in a sandstone/diatomaceous shale member of the Modelo formation. Concentrations that exceed the BTV cannot be attributed to SSFL without first considering local geology and the concentration depth profile.

As observed by US EPA, the background sample in the Santa Susana formation (location 2) had higher ^{232}Th concentrations compared to background samples in the Chatsworth formation, but the difference was not statistically significant. Thorium-232 concentrations in the samples taken for this project were statistically higher overall in the Santa Susana and Chatsworth formations (43.8 to 49.2 Bq kg^{-1}) compared to the Modelo, Calabasas, and Towsley formations (13 to 31.6 Bq kg^{-1}).

Soil concentration profiles

Soil concentration profiles were constructed to examine in more detail the concentration distribution with depth for those samples that exceeded the BTV values. Soil concentration profiles are important because airborne particles deposit on the soil surface so that concentrations in the surface layer would be higher than subsurface layers, as observed for ^{137}Cs from past global fallout (Rood et al. 2008; Zheng et al. 2012). The soil profiles for locations outside the deposition plume (locations 5 and 11 in Fig. 11) show the sample locations are undisturbed based on the ^{137}Cs profile whereas sample location 18, which was in the plume, showed evidence of past disturbance based on the ^{137}Cs depth profile. Sample location 5, which US EPA concluded shows no influence from SSFL and was in the Chatsworth formation, exhibited the highest concentration of ^{137}Cs in the surface soil and the most dramatic falloff with depth. Sample location 5 was within the China Flats region of the Santa Susana Mountains, which is a closed basin with little opportunity for erosion or sediment reworking. Consequently, most of the ^{137}Cs from fallout remained in the surface layer. Location 5 was also the only location that had detectable concentrations of ^{90}Sr. What is of particular importance at this location was the variability of ^{226}Ra, ^{230}Th, and ^{238}U in the different sampling depths. This location is undisturbed as demonstrated by the ^{137}Cs profile and outside any influence from SSFL. Ratios of the maximum concentration to minimum concentration ranged from 1.14 (^{226}Ra) to 1.23 (^{238}U). Thus, variability among the layers, with some layers being higher than the others, would be expected in the natural environment. In contrast, the ^{137}Cs maximum-to-minimum ratio (1.84 to 8.62) was higher for all sample locations that showed no evidence of disturbance compared to maximum-to-minimum ratios for uranium decay series.

Sample location 11 exhibited the highest concentrations of the uranium decay series. The sample was taken

Table 12. Soil sampling results for Priority-1 radionuclides that had two or more detections in a soil profile. Bolded entries are weighted-average concentrations that are statistically above (see eqn 7) the BTV.

Radionuclide	Loc	BTV (Bq kg^{-1})	Wt Avg (Bq kg^{-1})	Uncertainty (Bq kg^{-1})	Exceeds BTV	Radionuclide	Loc	BTV (Bq kg^{-1})	Wt Avg (Bq kg^{-1})	Uncertainty (Bq kg^{-1})	Exceeds BTV
Cs-137	1	5.94	1.64	0.44	No	Th-230	16	75.5	59.9	7.57	No
Cs-137	2	5.94	2.09	0.53	No	Th-230	17	75.5	15.3	4.37	No
Cs-137	3	5.94	2.90	0.45	No	Th-230	18	75.5	73.3	9.68	No
Cs-137	4	5.94	1.04	0.39	No	Th-232	1	112	46.8	7.35	No
Cs-137	5	5.94	4.50	0.67	No	Th-232	2	112	49.2	7.45	No
Cs-137	6	5.94	2.52	0.45	No	Th-232	3	112	46.9	6.66	No
Cs-137	8	5.94	1.64	0.44	No	Th-232	4	112	43.8	6.80	No
Cs-137	9	5.94	3.24	0.41	No	Th-232	5	112	48.9	6.81	No
Cs-137	10	5.94	4.30	0.26	No	Th-232	6	112	24.0	4.98	No
Cs-137	11	5.94	0.85	0.31	No	Th-232	8	112	28.9	9.26	No
Cs-137	13	5.94	2.82	0.39	No	Th-232	9	112	24.4	5.27	No
Cs-137	14	5.94	2.49	0.43	No	Th-232	10	112	14.2	3.88	No
Cs-137	15	5.94	2.84	0.47	No	Th-232	11	112	28.1	7.19	No
Cs-137	16	5.94	2.00	0.46	No	Th-232	13	112	31.6	5.45	No
Cs-137	17	5.94	1.24	0.18	No	Th-232	14	112	25.8	4.75	No
Cs-137	18	5.94	3.12	0.41	No	Th-232	15	112	27.0	5.24	No
Ra-226	1	69.3	42.2	1.44	No	Th-232	16	112	28.8	5.33	No
Ra-226	2	69.3	51.0	1.95	No	Th-232	17	112	13.1	3.88	No
Ra-226	3	69.3	54.0	1.93	No	Th-232	18	112	31.6	6.97	No
Ra-226	4	69.3	40.4	1.37	No	U-233/234	1	69.2	35.9	4.29	No
Ra-226	5	69.3	46.1	2.12	No	U-233/234	2	69.2	32.1	4.20	No
Ra-226	6	69.3	33.8	1.33	No	U-233/234	3	69.2	54.9	5.64	No
Ra-226	**8**	**69.3**	**76.6**	**1.90**	**Yes**	U-233/234	4	69.2	36.8	4.42	No
Ra-226	9	69.3	47.4	1.47	No	U-233/234	5	69.2	39.8	5.33	No
Ra-226	10	69.3	43.4	0.90	No	U-233/234	6	69.2	31.4	4.12	No
Ra-226	**11**	**69.3**	**105**	**1.64**	**Yes**	U-233/234	8	69.2	80.8	6.43	No
Ra-226	**13**	**69.3**	**79.6**	**1.67**	**Yes**	U-233/234	9	69.2	37.3	5.16	No
Ra-226	14	69.3	56.4	1.73	No	U-233/234	10	69.2	57.7	6.32	No
Ra-226	15	69.3	47.7	1.55	No	**U-233/234**	**11**	**69.2**	**116**	**8.26**	**Yes**
Ra-226	16	69.3	57.8	1.65	No	U-233/234	13	69.2	35.2	5.46	No
Ra-226	17	69.3	12.9	0.54	No	U-233/234	14	69.2	27.9	4.10	No
Ra-226	18	69.3	67.6	1.72	No	U-233/234	15	69.2	23.4	3.41	No
Ra-228	1	85.1	61.9	2.70	No	U-233/234	16	69.2	39.8	4.58	No
Ra-228	2	85.1	64.3	3.37	No	U-233/234	17	69.2	10.4	2.55	No
Ra-228	3	85.1	68.4	3.62	No	U-233/234	18	69.2	34.7	4.21	No
Ra-228	4	85.1	56.6	2.58	No	U-235/235	1	4.81	2.79	1.47	No
Ra-228	5	85.1	63.1	4.72	No	U-235/235	2	4.81	2.50	1.44	No
Ra-228	6	85.1	36.1	2.39	No	U-235/235	3	4.81	4.93	1.90	No
Ra-228	8	85.1	37.2	2.58	No	U-235/235	4	4.81	4.77	1.79	No
Ra-228	9	85.1	34.2	2.36	No	U-235/235	6	4.81	2.16	0.93	No
Ra-228	10	85.1	16.7	1.37	No	U-235/235	8	4.81	6.54	1.90	No
Ra-228	11	85.1	54.4	2.42	No	U-235/235	9	4.81	4.37	1.41	No
Ra-228	13	85.1	43.8	2.52	No	U-235/235	10	4.81	4.49	1.92	No
Ra-228	14	85.1	38.5	2.66	No	U-235/235	11	4.81	8.69	2.51	No
Ra-228	15	85.1	38.8	2.56	No	U-235/235	15	4.81	1.74	0.82	No
Ra-228	16	85.1	35.8	2.66	No	U-235/235	16	4.81	7.46	2.06	No
Ra-228	17	85.1	14.6	1.06	No	U-235/235	18	4.81	1.81	0.88	No
Ra-228	18	85.1	46.1	2.40	No	U-238	1	62.2	38.9	4.42	No
Sr-90	5	2.29	0.718	0.22	No	U-238	2	62.2	34.8	4.34	No
Th-230	1	75.5	42.9	7.15	No	U-238	3	62.2	55.0	5.66	No

Continued next page

Table 12. *(Continued)*

Radionuclide	Loc	BTV (Bq kg^{-1})	Wt Avg (Bq kg^{-1})	Uncertainty (Bq kg^{-1})	Exceeds BTV	Radionuclide	Loc	BTV (Bq kg^{-1})	Wt Avg (Bq kg^{-1})	Uncertainty (Bq kg^{-1})	Exceeds BTV
Th-230	2	75.5	35.2	6.65	No	U-238	4	62.2	35.1	4.36	No
Th-230	3	75.5	50.1	6.86	No	U-238	5	62.2	40.5	5.37	No
Th-230	4	75.5	36.8	6.19	No	U-238	6	62.2	31.5	4.20	No
Th-230	5	75.5	43.4	6.50	No	**U-238**	**8**	**62.2**	**82.0**	**6.45**	**Yes**
Th-230	6	75.5	38.8	6.44	No	U-238	9	62.2	34.8	4.84	No
Th-230	8	75.5	96.7	16.43	No	U-238	10	62.2	58.6	6.38	No
Th-230	9	75.5	76.1	9.07	No	**U-238**	**11**	**62.2**	**116.2**	**8.30**	**Yes**
Th-230	10	75.5	58.3	7.86	No	U-238	13	62.2	36.8	5.60	No
Th-230	**11**	**75.5**	**106**	**13.80**	**Yes**	U-238	14	62.2	26.1	3.95	No
Th-230	13	75.5	83.0	8.72	No	U-238	15	62.2	23.5	3.37	No
Th-230	14	75.5	49.1	6.56	No	U-238	16	62.2	47.1	4.92	No
Th-230	15	75.5	39.1	6.27	No	U-238	17	62.2	11.4	2.62	No

on top of a hill so some erosion could have occurred, but the ^{137}Cs profile still exhibited a noticeable decrease in concentration with depth, whereas the uranium decay series radionuclide did not. This indicates that the higher concentration in this area is a result of the local geology and not from any atmospheric deposition. The sample was taken in a sandstone/diatomaceous shale member of the Modelo formation that likely contained higher concentrations of natural uranium.

Locations 8, 9, and 10 would have received deposition from the fire burning across the Area I burn pit, but these samples showed no discernable elevated levels of ^{226}Ra in surface soils. Location 8 (in the Modelo formation) had notably higher levels of uranium decay series radionuclides at all depths compared to locations 9 (Modelo) and 10 (Towsley), but variation of concentration among the depths sampled was less than observed for background samples and indicates the higher concentrations are related to geologic natural variability and not atmospheric deposition.

Sample locations in the deposition plume (Fig. 12) also showed the effects of local geology and geomorphology. No evidence of atmospheric deposition from the Woolsey Fire was found in these samples. Sample locations 13 and 15 were taken in Palo Comado Canyon on the edge of the flood

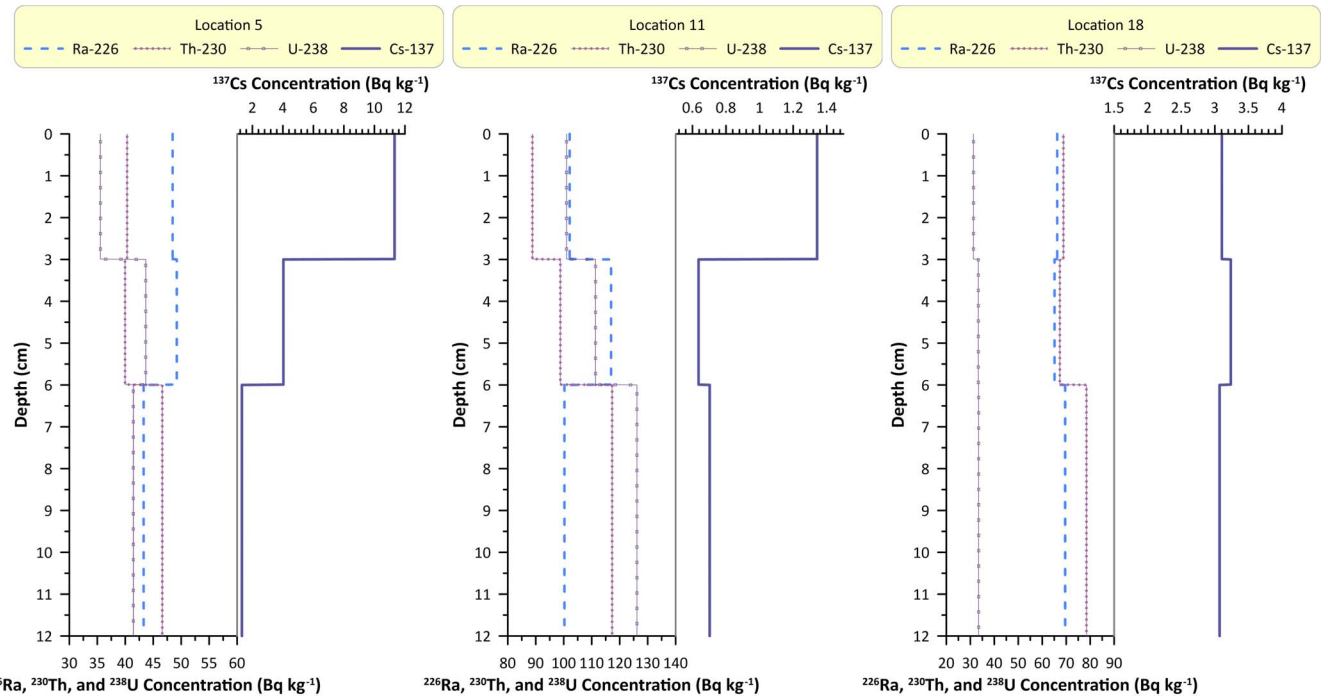

Fig. 11. Soil profiles of ^{137}Cs, ^{226}Ra, ^{230}Th, and ^{238}U at sampling locations outside the Woolsey Fire deposition plume (locations 5 and 11) and inside the deposition plume (location 18). Note that the ^{226}Ra, ^{230}Th, and ^{238}U concentrations are on the lower axis and the ^{137}Cs concentrations are on the upper axis.

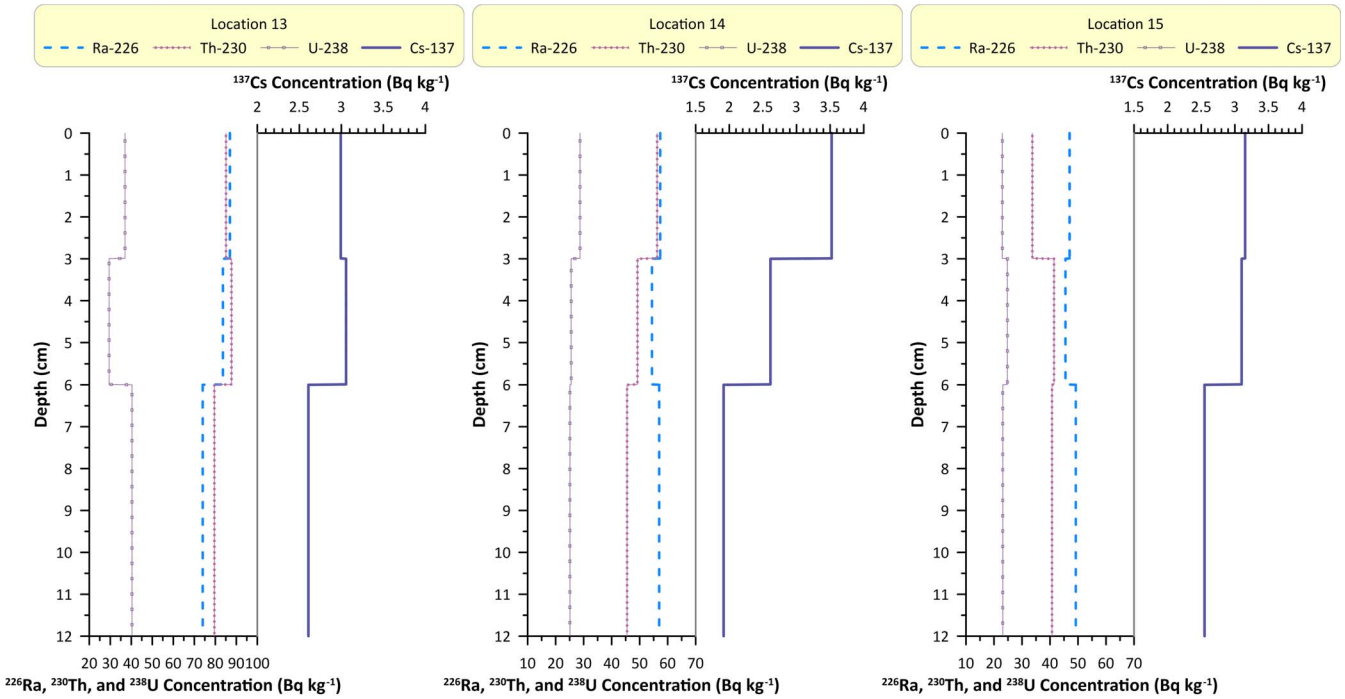

Fig. 12. Soil profiles of ^{137}Cs, ^{226}Ra, ^{230}Th, and ^{238}U at sampling locations in the deposition plume. Note that the ^{226}Ra, ^{230}Th, and ^{238}U concentrations are on the lower axis and the ^{137}Cs concentrations are on the upper axis.

plain. The ^{137}Cs profiles indicated some sediment reworking probably due to past flooding. Uranium decay series radionuclides exhibit expected variability among the layers, although ^{238}U had noticeably higher concentrations in the 6–12 cm layer than the 3–6 cm layer at location 13. Radium-226 had higher concentrations in the surface soil layer than at depth. If the ^{226}Ra depth profile observed at location 13 was from plume deposition, then we would expect to see similar depth profiles at locations 14, 15, and 18, all of which were located less than a kilometer from location 13. This was not observed. Sample location 13 had higher uranium decay series concentrations, which may be the result of its proximity to outcrops of the Calabasas formation and alluvial deposits.

Sample location 14 was taken on a flat area along the ridge east of the canyon. The ^{137}Cs depth profile is consistent with global fallout and the variability of uranium decay series radionuclides with depth was in the expected range for background. Like ^{226}Ra in sample 13, ^{230}Th had higher

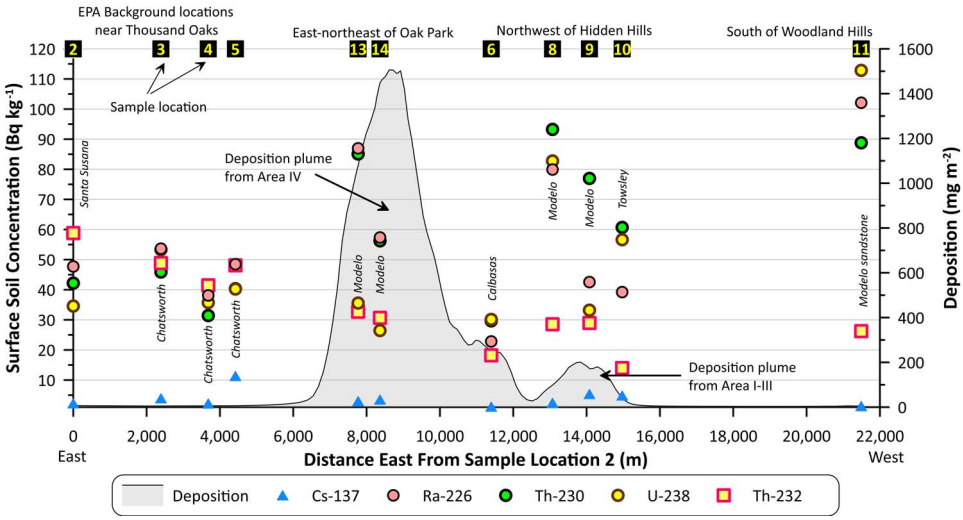

Fig. 13. East to west transect showing radionuclide concentrations in soil samples (left axis) and predicted deposition from plumes (gray-shaded region, right axis). Radionuclides displayed were detected in 0–3 cm layer at all sample locations. The geologic formations (see Fig. 9) for each sample are in italics.

concentrations in the surface soil than at depth. If the ^{230}Th depth profile observed at location 14 was from plume deposition, then we would expect to see similar depth profiles at locations 13, 15, and 18, all of which were located less than a kilometer from location 13, but this was not observed.

DISCUSSION

Another way to view the results is to plot a cross section across the deposition plume (Fig. 13). The cross-section line is illustrated in Fig. 5. The deposition plume cross section and measured radionuclide concentrations in the 0–3 cm layer for priority-1 radionuclides that were positively detected at all locations in the cross section show that (1) there are no discernable trends in anthropogenic radionuclide concentrations that would correspond to deposition from the plume; and (2) concentrations for some naturally occurring radionuclides are related to the geology.

Shortly after the Woolsey Fire, the California Environmental Protection Agency (CalEPA) and Department of Toxic Substances Control (DTSC) produced an interim and final report evaluating impacts of the Woolsey Fire on surrounding communities (DTSC 2018, 2020). The report summarized sampling work done between 8 and 30 November 2018 to address community concerns about the possibility that the Woolsey Fire caused radionuclides and hazardous materials on-site to migrate into surrounding communities. The report presented available soil/ash and air sampling data, mostly for hazardous materials, but also some radionuclide measurements and exposure rates. Based on different lines of evidence including modeling and measurements, DTSC concluded that no radiation or hazardous materials originating from the SSFL were detected in communities following the Woolsey Fire.

Following the Woolsey Fire, Kaltofen et al. (2021) performed a study of community-based sampling of ash, dust, and soil at various locations around SSFL. Although the authors conclude that there is evidence of decreasing radioactivity with increasing distance from SSFL and imply that high concentrations measured as part of the study are attributable to SSFL, the information provided in the article does not support this, and the data provided are insufficient to enable readers to reproduce or validate their findings. When the count rate data presented in Tables 1 and 2 of Kaltofen et al. (2021) are plotted as a function of distance from SSFL, there is no apparent trend in the data, and the highest values are seen at the most distant location. Their finding that 97% of the samples collected matched existing background levels was an important conclusion of the study, but without the spatial context of these samples relative to the samples with elevated activity, it is impossible to adequately interpret the data. The bio-tape sampling method used does not enable a depth profile comparison, which is fundamental to determining whether material has been deposited from the atmosphere and whether elevated activity levels were merely the result of a heterogenous environment where background levels can vary depending on the local geology.

Kaltofen et al. (2021) suggests that monazite particles (a rare earth phosphate mineral that contains thorium) that were detected in the samples originated from past SSFL activities but also mentions the possibility that exposed bedrock could be a source of the monazite. The thorium content of the monazite particles identified by Kaltofen et al. 2021 (2.1–9.6%) was in the range that is typically found in natural monazite deposits (3.1–11.3%; Salehuddin et al. 2019). The thorium used at SSFL would have been in the form of a metal oxide and not within the crystal lattice of a naturally occurring monazite mineral. Monazite is formed from igneous and metamorphic processes on geologic time scales. Monazite eroded from igneous or metamorphic source rock can concentrate in fluvial, deltaic, beach, or shallow water sediments due to its hardness and high specific gravity (4.6 to 5.4 g cm^{-3}) (King 2022). Sedimentary rocks formed from these processes are found in the SSLF region. Monazite has never been used or processed at the SSFL. Thus, the thorium in the monazite particles detected by Kaltofen et al. (2021) is associated with natural materials and processes and is not from any past activities on the SSFL.

Finally, an ash sample concentration cannot be compared directly to a soil sample concentration without correcting for the equivalent concentration in the unburned vegetation and the relationship between the concentration in unburned vegetation to that of soil. Thus, the conclusions drawn by Kaltofen et al. (2021) are not supported by the data and should be interpreted with caution.

CONCLUSION

Air measurement data collected during the Woolsey Fire, along with atmospheric dispersion modeling and an offsite soil sampling program designed specifically to look for impacts from the fire, showed no evidence of SSFL impact in off-site soils because of the Woolsey Fire. Variations in anthropogenic and naturally occurring radionuclides in soil was attributed to the underlying geologic formations and geomorphology of the sampling location.

Computer modeling of the fire progression identified the Oak Park community as the residential area that had the highest $PM_{2.5}$ air concentrations and deposition while the Woolsey Fire burned on the SSFL. Oak Park is located about 6 km southwest of the SSFL, and there was no evidence of SSFL-derived radionuclides in the soils collected in this area. The confirmatory soil sampling had the ability to detect doses from atmospheric deposition of radionuclides during the Woolsey Fire that ranged from 8.2×10^{-5} mSv for ^{90}Sr to 2.4×10^{-2} mSv for ^{234}U. These minimum detectable

doses are substantially less than regulatory limits or doses received from natural background. The amount of activity released from the Woolsey Fire necessary to detect radionuclides in soil at Oak Park based on the modeling is greater than the surface soil inventory in Area IV at SSFL. As such, even if the entire surface soil inventory were released, annual hypothetical doses at the Oak Park community would be less than 0.0002 mSv. Soil sampling within and outside the deposition plume confirmed that no detectable levels of SSFL-derived radionuclides migrated from SSFL because of the Woolsey Fire. Moreover, no evidence was found of impacts to off-site soils from past operations at the SSFL that may have resulted in releases to the atmosphere.

Acknowledgments—Source of funding: The Boeing Company.

REFERENCES

Atomics International. Environmental monitoring annual report for 1959. Los Angeles: Atomic International; 1960.

Anderson GK, Sandberg DV, Norheim RA. Fire Emission Production Simulator (FEPS) user's guide. USDA Forest Service Pacific Northwest Research Station, Joint Fire Science Program (98-1-9-05). Seattle, WA: USDA; 2004. Available at ***http://www.fs.fed.us/pnw/fera/feps/***. Accessed.

Bevington PR, Robinson DK. Data reduction and error analysis for the physical sciences. New York: McGraw-Hill Inc; 1992.

Boeing. Rocketdyne Propulsion & Power DOE Operations Annual Site Environmental Report 1997. Simi Valley, CA: Boeing; A4CM-ZR-0012; 1998.

Boeing. Site environmental report for calendar year 2000, DOE operations at The Boeing Company Rocketdyne Propulsion & Power. RD01-152; 2001.

Boeing. Site environmental report for calendar year 2004, DOE operations at The Boeing Company Santa Susana Field Laboratory. Simi Valley, CA: Boeing; RD05-176; 2005.

Boeing. Site environmental report for calendar year 2005, DOE operations at The Boeing Company Santa Susana Field Laboratory. Simi Valley, CA: Boeing; 2006.

Boeing. Site environmental report for calendar year 2007, DOE operations at The Boeing Company Santa Susana Field Laboratory, Area IV. Simi Valley, CA: Boeing; 2008.

Boeing. [online]. 2021. Available at ***https://www.boeing.com/principles/environment/santa-susana/extraordinary-past.page#/energy***. Accessed 9 December 2021.

Carsel RF, Parrish RS. Developing joint probability distributions of soil water retention characteristics. Water Resources Res 25:755–769; 1988.

Chang JC, Hanna SR. Air quality model performance evaluation. Meteorol Atmospher Phys 87:167–196; 2004.

Citygate Associates LLC. City of Los Angeles: after action review of the Woolsey Fire incident. Folsom, CA: Citygate Associates LLC; 2019.

Deeming JE, Burgan RE, Cohen JD. The National Fire Danger Rating System—1978. Ogden, UT: USDA Forest Service, Intermountain Forest and Range Experiment Station; General Technical Report INT-39;1977.

Department of Toxic Substance Control. DTSC Interim Summary Report of Woolsey Fire. Sacramento, CA: California Environmental Protection Agency; 2018.

Department of Toxic Substance Control. DTSC Final Summary Report of Woolsey Fire. California Environmental Protection Agency. Sacramento, CA: DTSC; 2020.

Exponent. CALPUFF Version 7 users guide addendum. Maynard, MA: Exponent Inc; 2019.

Grogan HA, Aanenson JW, McGavran PD, Meyer KR, Mohler HJ, Mohler SS, Rocco JR, Rood AS, Till JE. Modeling of the Cerro Grande Fire at Los Alamos: an independent analysis of exposure, health risk, and communication with the public. In: Semkow TM, Pomme A, Jerome SM, Strom DJ, eds. Applied modeling and computations in nuclear science. ACS Symposium Series 945. Washington, DC: American Chemical Society; 2007: 71–92.

HydroGeologic, Inc. Final radiological background study report Santa Susana Field Laboratory Ventura County, California. Prepared for US Environmental Protection Agency Region 9. Ballston Lake, NY: HydroGeologic; EPA Contract No: EP-S3-07-05; 2011.

HydroGeologic, Inc. Final technical memorandum look-up table recommendations, Santa Susana Field Laboratory Area IV Radiological Study [online]. 2012. Available at ***https://www.dtsc-ssfl.com/files/lib_doe_area_iv/epaareaivsurvey/techdocs/65778_Final_Tech_Memo_Lookup_Table_Recommendations_112712.pdf***. Accessed 9 August 2019.

Kaltofen M, Gundersen M, Gundersen A. Radioactive microparticles related to the Woolsey Fire in Simi Valley, CA. J Environ Radioact 240:106755; 2021.

Kamboj S, Gnanapragasam E, Yu C. User's guide for RESRAD-ONSITE Code, Version 7.2. ANL/EVS/TM-18/1. Argonne, IL: Argonne National Laboratory; March 2018.

King HM. Monazite: a rare phosphate mineral mined from placer deposits for its rare earth and thorium content [online]. 2022. Available at ***https://geology.com/minerals/monazite.shtml***. Accessed 3 February 2022.

County LA. Los Angeles County GIS Data Portal [online]. 2019. Available at ***https://egis3.lacounty.gov/dataportal/2018/11/21/woolsey-fire-nov-2018-gis-data-applications/***. Accessed 19 June 2019.

Lambert G, Le Cloarec MF, Ardouin B, Bonsang B. Long-lived radon daughters signature of Savanna Fires. In: Levine JS, ed. Global biomass burning. Cambridge, MA: MIT Press; 1991: 181–184.

Le Cloarec MF, Ardouin B, Cachier H, Liousse C, Neveu S, Nho E-Y. ^{210}Po in Savanna burning plumes. J Atmospher Chem22: 111–122; 1995.

Moore JD. Rocketdyne Division Environmental Monitoring Annual Report, De Soto and Santa Susana Field Laboratories Sites 1985. Rockwell International; RI/RD86-140; 1986.

Moore JD. Rocketdyne Division Environmental Monitoring Annual Report, De Soto and Santa Susana Field Laboratories Sites 1989. Simi Valley, CA: Rockwell International; RI/RD90-132; 1990.

Nance JD, Hobbs PV, Radke LF. Airborne measurements of gases and particles from an Alaskan wildfire. J Geophys Res98:14, 873–14,882; 1993.

National Council on Radiation Protection and Measurements. Ionizing radiation exposure of population of the United States. Bethesda, MD: NCRP; NCRP Report No. 160; 2009.

North Wind, Inc. Annual Site Environmental Report for Calendar Year 2014, Department of Energy Operations at the Energy Technology Engineering Center—Area IV Santa Susana Field Laboratory. Idaho Falls, ID: North Wind Inc; 2015.

North Wind, Inc. Annual Site Environmental Report for Calendar Year 2017, Department of Energy Operations at the Energy Technology Engineering Center—Area IV Santa Susana Field Laboratory. Idaho Falls, ID: North Wind Inc; 2018.

North Wind, Inc. Radioactive particulate air sampling results associated with the Woolsey Fire. Idaho Falls, ID: North Wind Inc; 2019a.

North Wind, Inc. Report on Quarterly Air Monitoring, Area IV, Third Quarter 2018–2019. Santa Susana Field Laboratory, Ventura County, California. Idaho Falls, ID: North Wind Inc; 2019b.

Ornduff R, Introduction to California plant life. Berkeley, CA: University of California Press; 1974.

Rockwell International. Rocketdyne Division Environmental Monitoring Annual Report Santa Susana Field Laboratory, De Soto, and Canoga Sites 1990. Simi Valley, CA: Rockwell Inernational; RI/RD91-136; 1991.

Rockwell International. Rocketdyne Division Environmental Monitoring Annual Report Santa Susana Field Laboratory, De Soto, and Canoga Sites 1991. Simi Valley, CA: Rockwell International; RI/RD92-138; 1992.

Rockwell International. Rocketdyne Division Environmental Monitoring Annual Report Santa Susana Field Laboratory, De Soto, and Canoga Sites 1993. Simi Valley, CA: Rockwell International; RI/RD94-126; 1994.

Rood AS, Voilleque PG, Rope SK, Grogan HA, Till JE. Reconstruction of atmospheric concentrations and deposition of uranium and decay products released from the former uranium mill at Uravan, Colorado. J Environ Radioact 99:1258–1278; 2008.

Rood AS, Mohler HJ, Grogan HA, Caffrey EA, Mangini C, Till JE. Evaluation of off-site impacts from the Woolsey Fire burning on portions of the Santa Susanna Field Laboratory Site. Neeses, SC: Risk Assessment Corporation; 01-SSFL-2020 FINAL; 2020.

Salehuddin AHJM, Ismail AF, Bahri CNACZ, Aziman ES. Economic analysis of thorium extraction from monazite. Nucl Engineer Technol51:631–640; 2019. DOI:10.1016/j.net.2018.11.005.

Scire JS, Strimaitis DG, Yamartino RJ. A user's guide for the CALPUFF dispersion model (Version 5). Concord, MA: Earth Tech Inc.; 2000. Available at ***http://www.src.com/calpuff/download/CALPUFF_UsersGuide.pdf***. Accessed 17 July 2014.

Turner DB. A diffusion model for an urban area. J Appl Meteorol 3: 83–91; 1964.

US Department of Energy. Derived concentration technical standard. Washington, DC: US Department of Energy; DOE-Std-1196-2021; 2021.

US Department of Energy. Radiation protection of the public and enviroment. Washington, DC: USDOE; DOE O 458.1 Chg 4; 15 September 2020.

US Environmental Protection Agency. External exposure to radionuclides in air, water, and soil: Federal Guidance Report 15. Washington, DC: US Environmental Protection Agency, Office of Radiation and Air; EPA-402/R19/002; 2019.

Webb SB, Ibrahim SA, Whicker FW. A three-dimensional spatial model of plutonium in soil near Rocky Flats, Colorado. Health Phys73:340–349; 1997.

Whicker FW, Rood AS. Terrestrial food chain pathways. In: Till JE, Grogan HA, eds. Radiological risk assessment and environmental analysis. New York: Oxford University Press; 2008: 260–339.

Wildfire Today. Woolsey Fire news [online]. 2019. Available at ***https://wildfiretoday.com/?s=Woolsey+Fire&monthnum=11&year=2018&states_provinces=*** 111&countries = &topics=. Accessed 19 June 2019.

Yerks RF, Campbell RH. Preliminary geologic map of the Los Angeles 30′ × 60′ Quadrangle, Southern California. Washington, DC: US Department of the Interior, Geologic Survey; USGS Open File Report 2005-1019; 2005.

Zheng J, Tagami K, Watanabe Y, Uchida S, Aono T, Ishii N, Yoshida S, Kubota Y, Fuma S, Ihara S. Isotopic evidence of plutonium release into the environment from the Fukushima DNPP accident. Scientific Reports 2:304; 2012. DOI:10.1038/srep00304.

■■